Electronic Supplementary Material (ESI) for ChemComm.

Supplemental Information

Engineered fluorogenic HaloTag ligands for *turn-on* labelling in live cells

Bryan J. Lampkin and Joshua A. Kritzer

Department of Chemistry, Tufts University, Medford MA 02155

Table of Contents

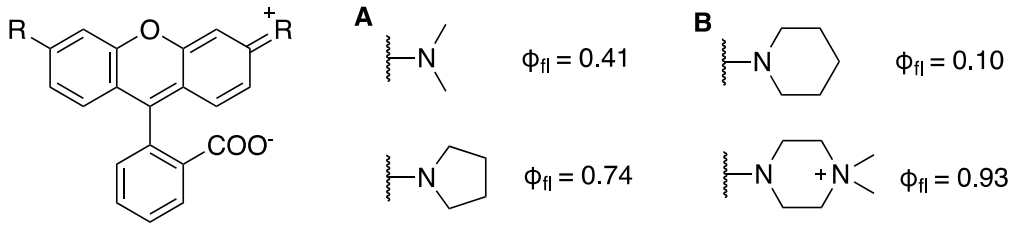

Figure S1. Representative examples of inconsistencies between two models of inhibiting TICT: decreasing the C—N—C bond angle and decreasing the electron-donating character of the conjugated amine. (A) Pyrrolidine-substituted rhodamine has a larger quantum yield of fluorescence than the corresponding dimethylamine derivative despite pyrrolidine being a better electron donor (more susceptible to TICT, Table S1); data from ref. 1. (B) Piperidine-substituted rhodamines have a lower quantum yield of fluorescence than the corresponding quaternary piperazine derivative, which is a weaker electron donor. Both derivatives have similar endocyclic C—N—C bond angles; data from ref. 1 and 2, respectively.

Table S1 – Experimental Ionization Potentials of Substituted Amines

Entry	Substituted Amine	IP (eV)[a]	IP (eV)[b]	IP (eV)[c]
1	NH_3	10.85		
2	Dimethyl amine	8.93		
3	Diethyl amine	8.63		
4	Aziridine		9.85	
5	Azetidine		9.04	
6	Pyrrolidine	8.77	8.77	8.82
7	Piperidine	8.66	8.64	8.66
8	Morpholine			8.91
8	Trimethyl amine	8.53		
9	N-methyl diethyl amine	8.22		
10	N-Methyl Pyrrolidine	8.41	8.41	
11	N-Methyl Piperidine	8.29	8.29	

[a] Ionization potentials are reported in ref. 3
[b] Ionization potentials are reported in ref. 4
[c] Ionization potentials are reported in ref. 5

Protein Expression and Purification

Protein expression was performed as previously reported.[6] A plasmid encoding an N-terminal His6x-HaloTag fusion was transformed into NEB 5α E. Coli cells and grown on ampicillin selection LB/Agar plates overnight at 37 °C. Several colonies were inoculated into 10 mL of LB media supplemented with 100 µg/mL ampicillin (GoldBio) and grown overnight at 37 °C to saturation. The following morning, the 10 mL cultures were diluted to 1 L of LB media supplemented with 100 µg/mL ampicillin and grown at 37 °C until the cultures reached an OD_{600} of 0.6, after which cultures were induced with 1 mL of 1M isopropyl β-D-1-thiogalactopyranoside (IPTG). Induced cultures were left to incubate overnight at room temperature and then pelleted at 4,000 rpm at 4 °C. Pellets were lysed in a lysis buffer containing 50 mM Tris-Cl, 100 mM NaCl, 5 mM imidazole, and 0.1 mM EDTA, with 1 mg/mL lysozyme, 5 mM 2-mercaptoethanol, and protease inhibitor cocktail (Roche). Lysis was accomplished by sonicating the pellet on ice in lysis buffer for 10 minutes with a 30-second on/off cycle. Lysates were clarified by centrifugation at 10,000 rpm for 30 minutes at 4 °C, and the supernatant was purified by batch affinity purification using Ni-NTA resin. The Ni-NTA resin was first equilibrated with His-binding buffer (50 mM Tris-Cl, 100 mM NaCl, 5 mM imidazole, and 0.1 mM EDTA). The lysis supernatant was then added to the equilibrated resin and incubated at 4 °C for 1 hour. The flow through was discarded, and the resin was washed with His-wash buffer (50 mM Tris-Cl, 300 mM NaCl, 10 mM imidazole, and 0.1 M EDTA, 5 mM 2-mercaptoethanol). His6x-HaloTag was then eluted from the Ni-NTA resin with His-elution buffer (50 mM Tris-Cl, 50 mM NaCl, 300 mM imidazole, 0.1 mM EDTA, 2 mM 2-mercaptoethanol). Eluted fractions were combined and then desalted into PBS pH 7.4 to remove imidazole and 2-mercaptoethanol.

Photophysical measurements

Steady state photophysical measurements were conducted in aerated solvents at approximately 10 μM of dye such that the absorbance did not exceed 0.1. Quantum yield of fluorescence was calculated using eq. 1, where F is the integrated intensities, *f* is the overlap absorbance value between the dye and standard, and η is the refractive index of the solvent; *i* and s stand for sample and standard, respectively. Coumarin153 in ethanol was used as the standard ($\varphi_{Fl,\ standard}$ = 0.53).

$$(1)\ \Phi_{fl}^{i} = \left(\frac{F^{i} f_{s} \eta_{i}^{2}}{F^{s} f_{i} \eta_{s}^{2}}\right) \Phi_{fl}^{s}$$

Table S2 – Photophysical Properties of Dyes 1-5

	Solvent	λ_{abs} (nm) [a]	λ_{em} (nm)	log(ε)	Φ_{fl} [b]			Brightness (ε x Φ_{fl})
1	PBS	445	N.D	3.94	0.003	±	0	26
	Ethanol	449	568	3.85	0.073	±	0.0005	517
	Acetonitrile	448	580	3.91	0.082	±	0.018	667
	Dioxane	457	524	3.98	0.268	±	-	2559
	PBS + HaloTag7	451	529	3.88	0.425	±	0.064	3224
2	PBS	450	613	3.85	0.0035	±	0.001	1
	Ethanol	451	579	3.94	0.131	±	0.001	1141
	Acetonitrile	454	583	3.93	0.167	±	0.037	1421
	Dioxane	450	533	3.94	0.268	±	-	2334
	PBS + HaloTag7	456	534	3.87	0.531	±	0.009	3936
3	PBS	453	610	3.88	0.005	±	0.001	38
	Ethanol	453	567	4.03	0.165	±	0.001	1768
	Acetonitrile	451	574	4.05	0.142	±	0.038	1593
	Dioxane	451	528	3.92	0.394	±	-	3277
	PBS + HaloTag7	458	528	3.94	0.644	±	0.066	5609
4	PBS	444	600	3.88	0.003	±	0.001	23
	Ethanol	445	580	3.83	0.063	±	0.0025	426
	Acetonitrile	447	588	3.97	0.068	±	0.011	635
	Dioxane	446	540	3.97	0.145	±	-	1353
	PBS + HaloTag7	451	544	3.89	0.277	±	0.023	2150
5	PBS	419	604	3.87	0.007	±	0.001	52
	Ethanol	427	570	3.8	0.143	±	0.023	902
	Acetonitrile	425	583	3.98	0.157	±	0.013	1499
	Dioxane	438	535	3.83	0.262	±	-	1771
	PBS + HaloTag7	430	535	3.92	0.443	±	0.037	3685

[a] Absorbance was measured at 10 μM such that the absorbance did not exceed 0.1. [b] Quantum yields were measured using Coumarin153 (0.53) as a standard and calculated using equation **1**.

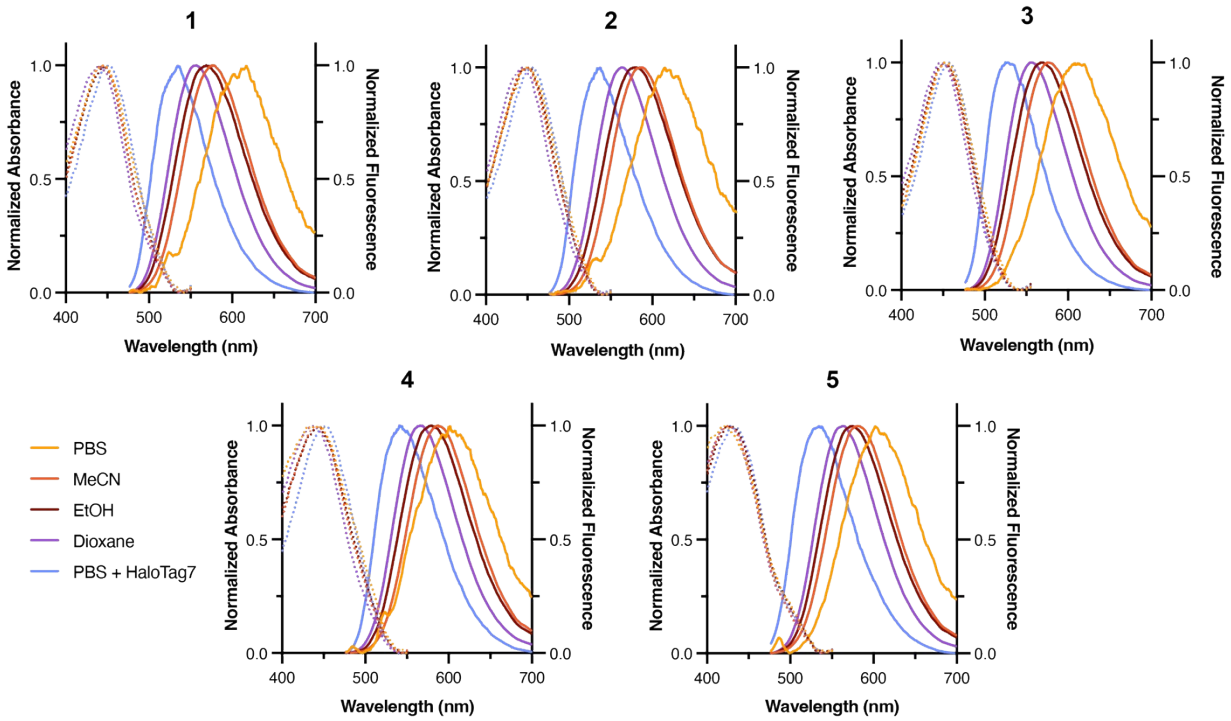

Figure S2. Normalized steady state absorbance (dotted traces) and fluorescence (solid traces) for **1-5** in different solvents.

HaloTag Labeling Kinetics

Dye conjugation rates to HaloTag were measured as described.[7] Briefly, 1.0 μM of dye were incubated with increasing concentrations of recombinant HaloTag. Dyes **1-4** were excited at 450 nm and emissions read at 535 nm. Dye **5** was excited at 430 nm and read at 535 nm. The time difference between addition of dye and the first measurement was accounted for in rate determination.

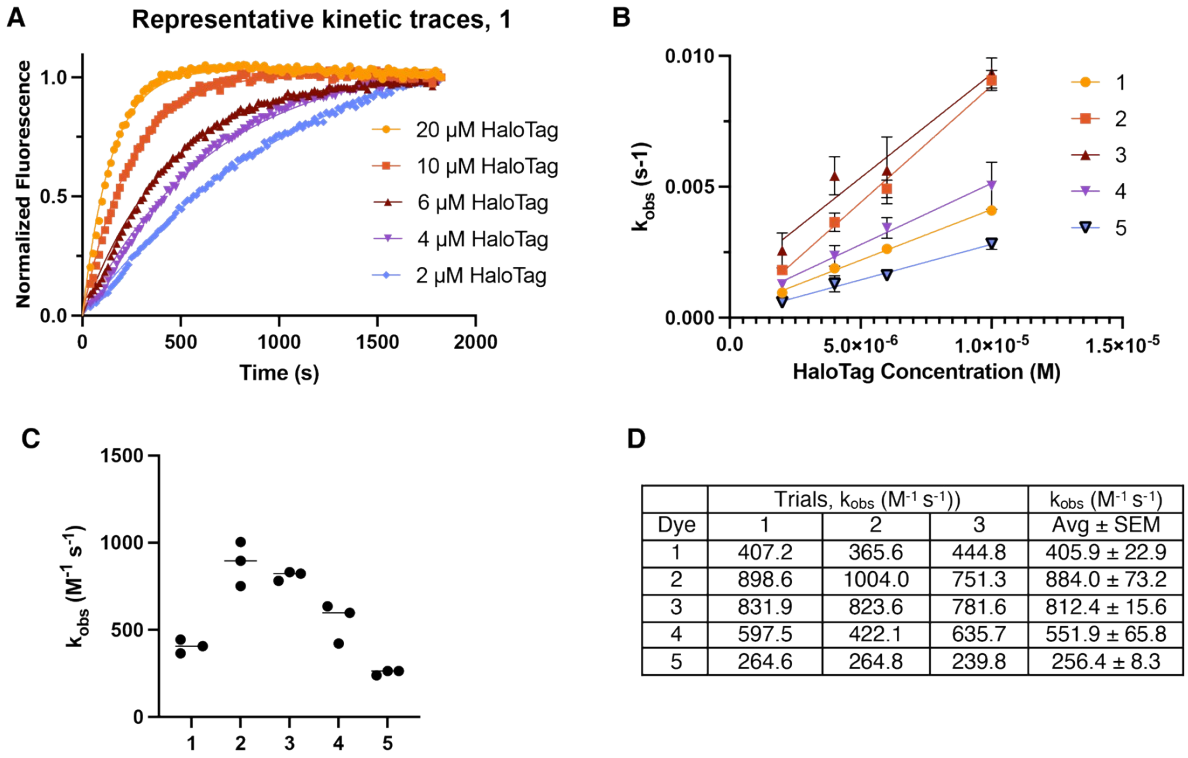

D

	Trials, k_{obs} (M^{-1} s^{-1}))			k_{obs} (M^{-1} s^{-1})
Dye	1	2	3	Avg ± SEM
1	407.2	365.6	444.8	405.9 ± 22.9
2	898.6	1004.0	751.3	884.0 ± 73.2
3	831.9	823.6	781.6	812.4 ± 15.6
4	597.5	422.1	635.7	551.9 ± 65.8
5	264.6	264.8	239.8	256.4 ± 8.3

Figure S3. Kinetic analysis of benzothiadiazole dyes. (A) Representative kinetic traces for **1** (0.5 μM) at varying concentrations of HaloTag (2-20 μM). Curves were fit using a one-phase association equation. (B) Plots of k_{obs} (s^{-1}) for **1-5** as a function of HaloTag concentration. (C) Summary of individual kinetic runs. (D) Raw data from three replicates.

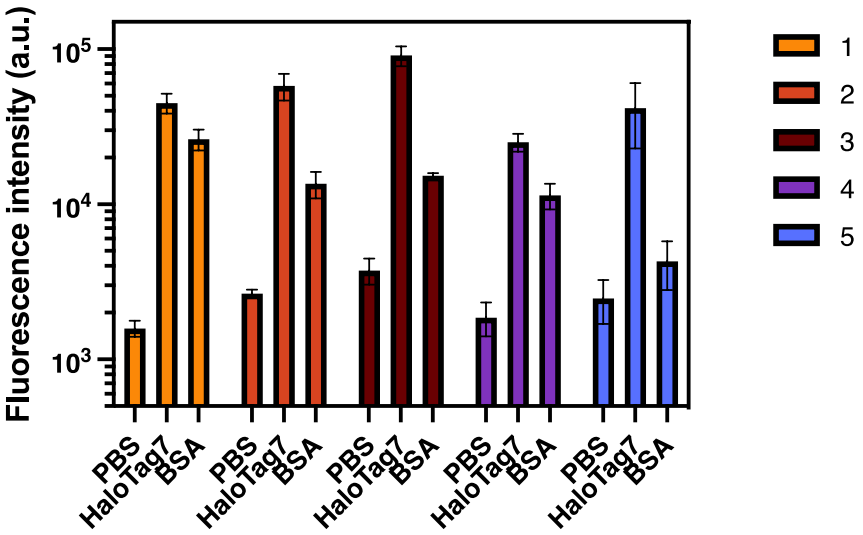

Figure S4. Raw fluorescence intensity values for **1-5** (2 μM) in buffer, buffer plus HaloTag7 (5 μM) or buffer plus bovine serum albumin (10 μM). Data shown is the mean maximum fluorescence intensities of at least three replicates.

Mammalian Cell Culture

HeLa cells were cultured in high-glucose DMEM with 10% fetal bovine serum 1% penicillin/streptomycin. All cells were transiently transfected using X-tremeGene 9 DNA transfection reagent (Roche) according to manufacturer instructions. Cells were transfected using a HaloTag7-mCherry fusion construct with a CMV promoter, generously gifted by X. Zhang.[7]

For microscopy experiments, $1x10^5$ cells were seeded two days prior to imaging in a 12-well plate and incubated overnight at 37 °C with 5% CO_2. The following day, cells were transfected approximately 18-24 hours prior to imaging. On the day of imaging, cells were aspirated and washed 1x with PBS and stained with Hoescht dye following manufacturer instructions. Cells were then treated with 500 μL of 1 μM dye in PBS buffer for 10 minutes and then imaged directly without aspiration of the dye solution.

For flow cytometry experiments, $1x10^4$ cells were seeded in a 96-well plate two days prior to analysis and incubated overnight at 37 °C with 5% CO_2. The following day, relevant wells were transfected approximately 18-24 hours prior to analysis. Each plate contained three technical replicate measurements for cells + dye, transfected cells + dye, and cells + DMSO (vehicle). On the day of analysis, each well was aspirated and washed once with PBS prior to treatment with 50 μL of 1 μM dye for either 10 or 60 minutes. After the allotted incubation time, wells were aspirated, directly trypsinized, and resuspended in PBS. The cells were analyzed by flow cytometry while gating for live, HaloTag-expressing (by measure of mCherry fluorescence) cells. All dyes were tested in three biological replicates at each time point.

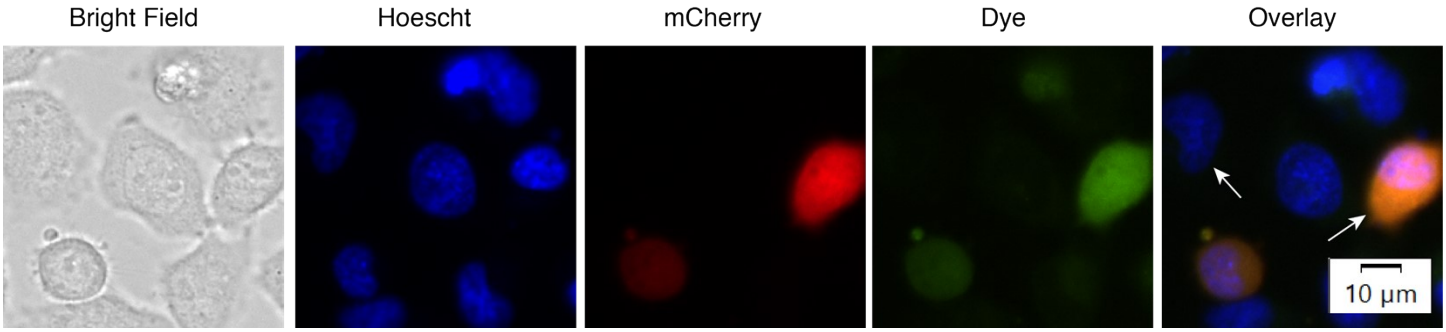

Figure S5. Bright field and fluorescence microscopy images of live HeLa cells transfected with HaloTag-mCherry and treated with **1**.

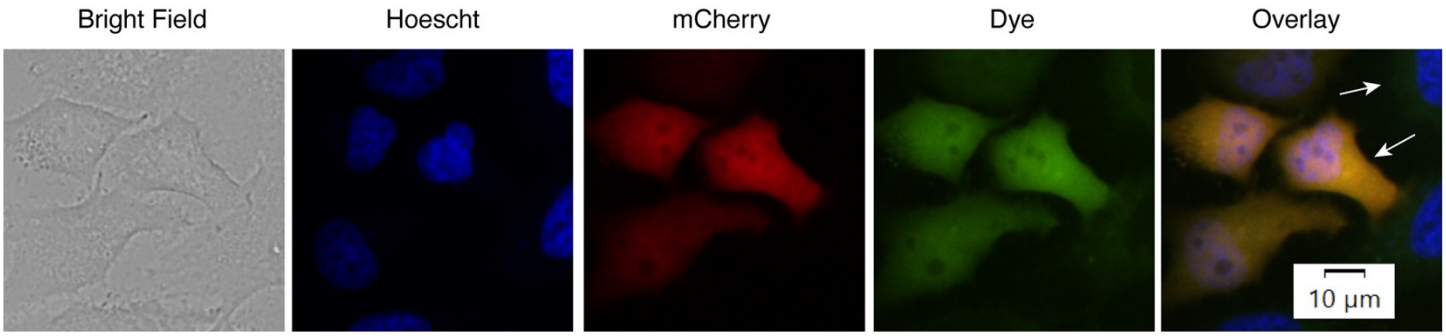

Figure S6. Bright field and fluorescence microscopy images live HeLa cells transfected with HaloTag-mCherry and treated with **2**.

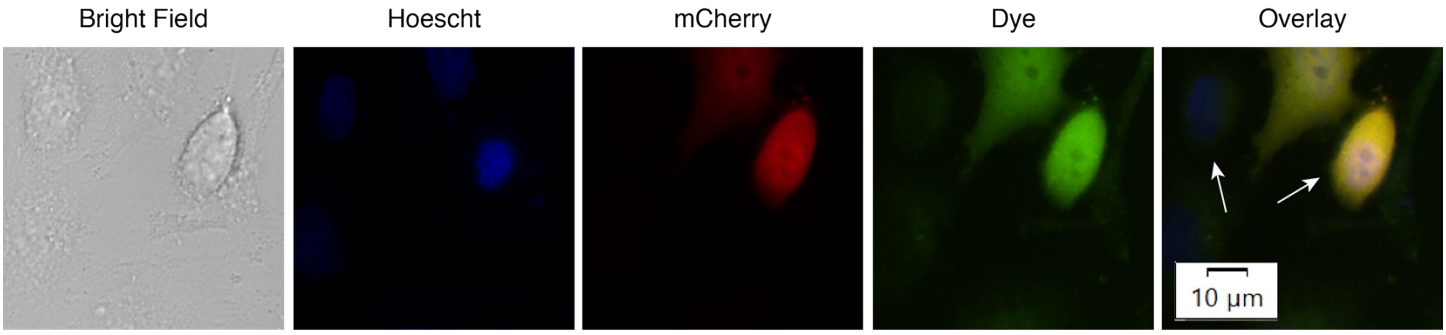

Figure S7. Bright field and fluorescence microscopy images of live HeLa cells transfected with HaloTag-mCherry and treated with **3**.

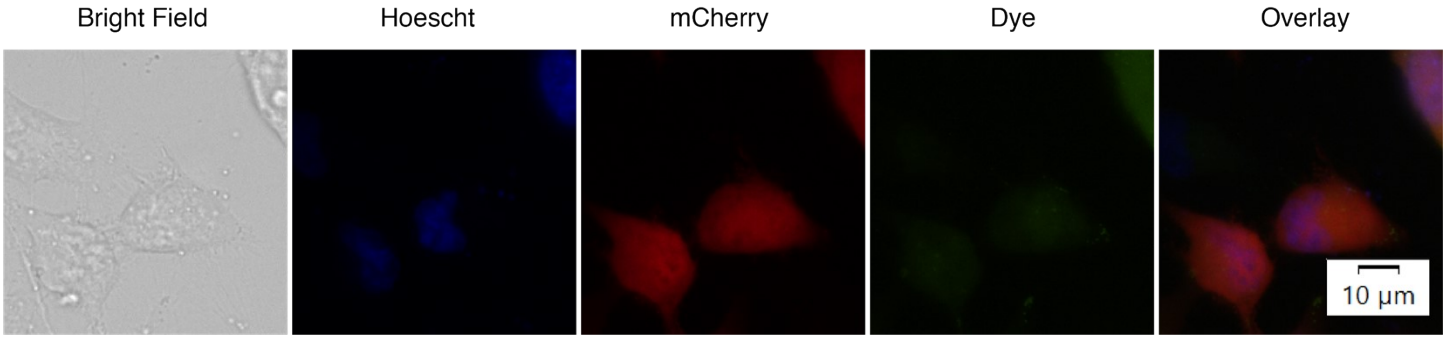

Figure S8. Bright field and fluorescence microscopy images of live HeLa cells transfected with HaloTag-mCherry and treated with **4**.

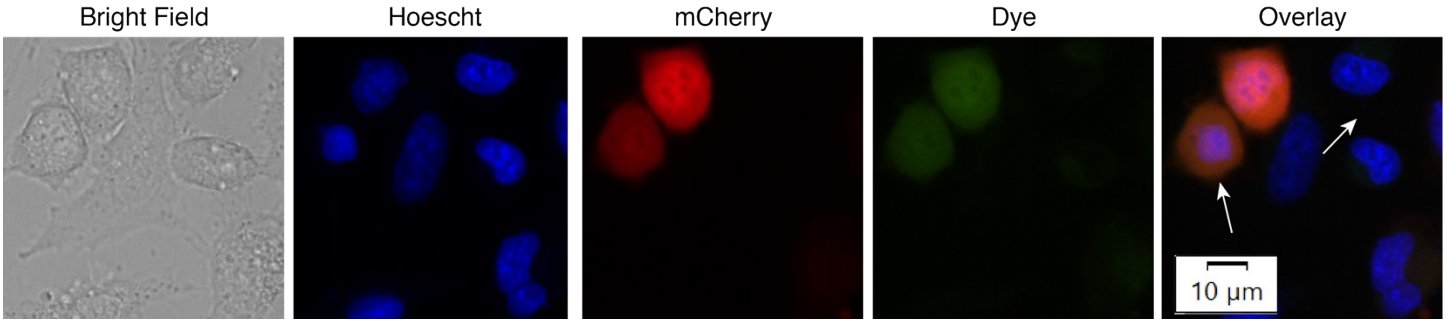

Figure S9. Bright field and fluorescence microscopy images of live HeLa cells transfected with HaloTag-mCherry and treated with **5**.

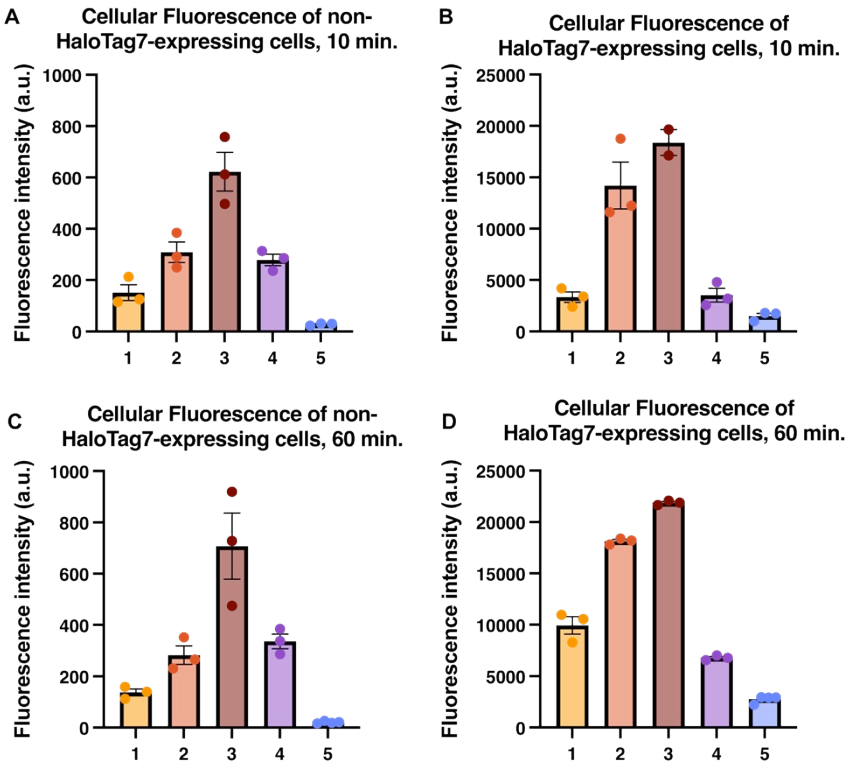

Figure S10. Mean fluorescence intensities of HeLa cells (A, C) or HaloTag7-expressing HeLa cells (B, D) treated with **1-5** for 10 or 60 minutes.

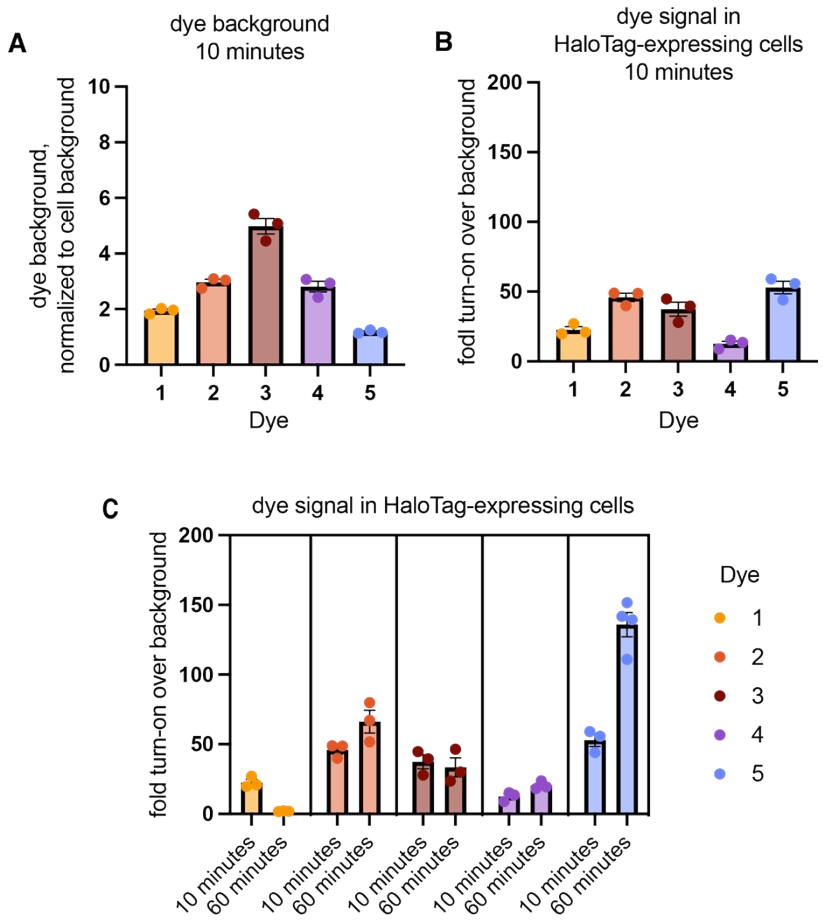

Figure S11. (A) Background fluorescence of each dye in non-HaloTag-expressing cells after 10 minutes of incubation, calculated as the ratio between the mean dye background (fluorescence of dye-treated, non-HaloTag-expressing cells) and the mean cell background (autofluorescence in non-dye-treated cells). (B) Turn-on fluorescence of each dye in live cells, calculated as the ratio of the mean dye signal (fluorescence of dye-treated, HaloTag-expressing cells) and the mean dye background (fluorescence of dye-treated, non-HaloTag-expressing cells). See Fig. 3 in main text for more details and analogous data for 60 minute incubation. (C) Head-to-head comparison of turn-on fluorescence of each dye in live cells after 10 or 60 minutes of incubation.

Synthesis

Scheme S1. Synthesis of benzothiadiazole dyes **1**-**5**.

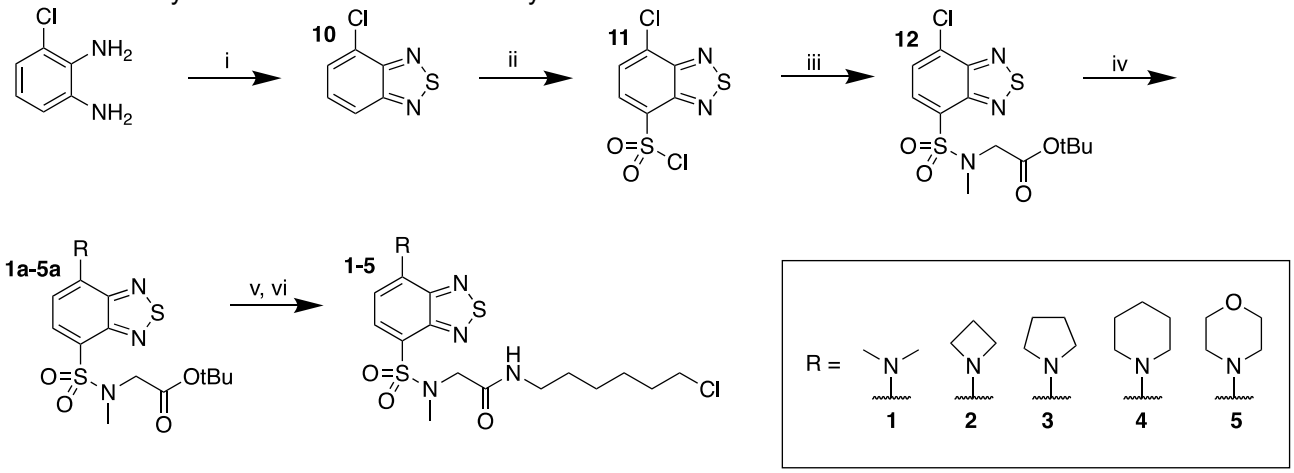

i. $SOCl_2$, triethylamine, CH_2Cl_2; *ii.* HSO_3Cl (neat); *iii.* Sarcosine•HCl, DIEA, CH_2Cl_2; *iv.* 4.0 eq. amine, DIEA, $CHCl_3$, 60 °C; *v.* 20% TFA/CH_2Cl_2; *vi.* IBCF, NMM, -78 °C, 30 min., 2.0 eq. 6-chlorohexylamine·HCl, -78 °C → room temperature, 12 hours.

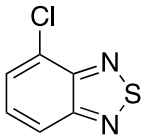

Synthesis of 10. Synthesized as previously described.[7] To a solution of 1,2-diamine-3-chlorobezene (19.7 mmol, 2.8 g) in dichloromethane (200 mL) was added triethylamine (79 mmol, 11.0 mL), followed by thionyl chloride ($SOCl_2$, 40 mmol, 2.4 mL) dropwise. The solution was refluxed at 50 °C for 6 hours. Upon completion, the reaction was quenched with 100 mL 1M HCl and the organic layer was collected. The organic layer was washed with brine (1x) and dried with sodium sulfate. The crude oil was purified by silica gel chromatography to yield the target compound as an off white solid (1.87 g, 56% yield). ^{1}H NMR (500 MHz, $CDCl_3$) δ 7.54 (dd, *J* = 7.45, 8.65 Hz, 1H), 7.64 (d, *J* = 7.1 Hz, 1H), 7.94 (d, *J* = 8.7 Hz, 1H); ^{13}C NMR (125 MHz, $CDCl_3$) δ 120.3, 126.1, 128.4, 129.5, 152.4, 155.3.

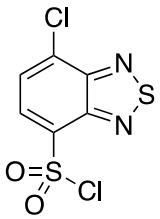

Synthesis of 11. Molecule 10 (8.8 mmol, 1.5 g) was dissolved in chlorosulfonic acid (10 mL) and heated to 140 °C. Upon completion, the solution was allowed to cool to room temperature and was quenched with 80 mL of DI water and back extracted with ethyl acetate (3x). The resulting organic layers were washed with brine (1x), dried over sodium sulfate, and concentrated to yield the target compound as an off white solid (1.02 g, 43% yield). The product was used without further purification.

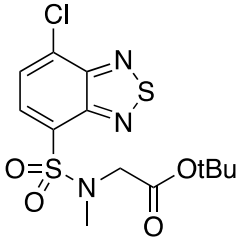

Synthesis of 12. Synthesized as previously described.[7] To a solution of **11** (3.0 mmol, 807 mg) in dichloromethane (30 mL) was added diisopropylamine (6.9 mmol, 1.23 mL) and sarcosine·HCl (3.0 mmol, 543 mg) and stirred at ambient temperature for 4 hours. Upon completion, quench with 1M HCl (30 mL) and back extract with dichloromethane (3x). The combine organic layers were washed with brine (1x), dried over sodium sulfate and concentrated. The resulting oil was purified by silica gel chromatography to yield the target compound as a white solid (966 mg, 85% yield). ^{1}H NMR (500 MHz, $CDCl_3$) δ 1.39 (s, 9H), 3.04 (s, 3H), 4.21 (s, 2H), 7.71 (d, *J* = 7.65 Hz, 1H), 8.18 (d, *J* = 7.65 Hz, 1H); ^{13}C NMR (125 MHz, $CDCl_3$) δ 27.9, 35.8, 82.1, 127.1, 130.8, 131.3, 131.5, 150.1, 152.9, 167.5; HRMS calculated: 400.0163 (M+Na), found: M+23 400.0196 (M+Na).

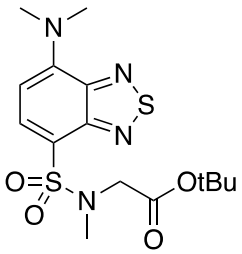

Synthesis of 1a. Representative procedure and synthesized as previously described.[7] To a solution of **12** (0.8 mmol, 300 mg) in dichloromethane (10 mL) was added 40% dimethylamine (8 mmol, 350 µL) and stirred vigorously for 18 hours. Upon completion, the reaction was quenched with 0.1M HCl (10 mL) and back extracted with dichloromethane (3x). The organic layers were combined, washed with brine (1x), dried over sodium sulfate and concentrated. The crude product was purified by silica gel chromatography to yield the target compound as an orange solid (XX mg, XX% yield). ^{1}H NMR (500 MHz, $CDCl_3$) δ 1.34 (s, 9H), 2.93 (s, 3H), 3.47 (s, 6H), 4.14 (s, 2H), 6.33 (d, *J* = 8.45 Hz, 1H), 8.05 (d, *J* = 8.4 Hz., 1H); ^{13}C NMR (125 MHz, $CDCl_3$) δ 27.92, 35.5, 42.61, 52.22, 81.53, 103.52, 135.09, 146.7, 147.9, 152.26, 168.22; HRMS calculated: 409.0975 (M+Na), found: 409.968 (M+Na).

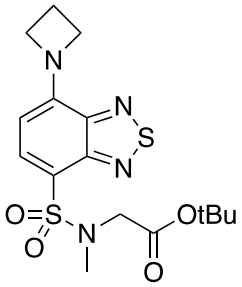

Synthesis of 2a. 0.2 mmol scale yielding an orange solid (68 mg, 86% yield). ^{1}H NMR (500 MHz, $CDCl_3$) δ 1.34 (s, 1H), 2.53 (m, 2H), 2.91 (s, 3H), 4.12 (s, 2H), 4.47 (s, 4H), 5.95 (d, *J* = 8.2 Hz., 1H), 8.00 (d, *J* = 8.2 Hz, 1H); ^{13}C NMR (125 MHz, $CDCl_3$) δ 17.1, 27.8, 35.36, 52.9, 81.4, 99.4, 114.6, 135.1, 145.26, 146.63, 151.83, 168.12,; HRMS calculated: 421.0975 (M+Na), found: 421.0984 (M+Na).

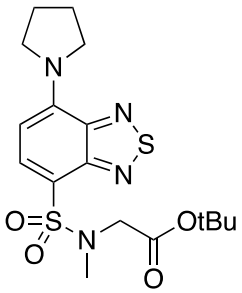

Synthesis of 3a. 0.2 mmol scale yielding an orange solid (81 mg, quantitative yield). ^{1}H NMR (500 MHz, $CDCl_3$) δ 1.34 (s, 9H), 2.07 (m, 4H), 2.89 (s, 3H), 3.89 (s, 4H), 4.12 (s, 2H), 6.14 (d, *J* = 8.5 Hz., 1H), 8.0 (d, *J* = 8.45 Hz., 1H); ^{13}C NMR (125 MHz, $CDCl_3$) δ 25.42, 27.79, 35.4, 50.69, 52.21, 81.42, 101.5, 113.88, 135.62, 144.07, 147.52, 152.23, 168.26; HRMS calculated: 435.1131 (M+Na), found: 435.1134 (M+Na).

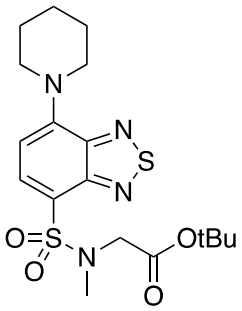

Synthesis of 4a. 0.2 mmol scale yielding an orange solid (71 mg, 83% yield). ^{1}H NMR (500 MHz, $CDCl_3$) δ 1.32 (s, 9H), 1.72 (m, 2H), 1.78 (m, 4H), 2.94 (s, 3H), 3.76 (m, 3H), 4.15 (s, 2H), 6.59 (d, *J* = 8.3 Hz., 1H), 8.06 (d, *J* = 8.25 Hz., 1H); ^{13}C NMR (125 MHz, $CDCl_3$) δ 24.5, 25.8, 28.0, 35.6, 50.9, 52.2, 81.7, 107.1, 119.1, 134.8, 147.6, 148.9, 152.0, 168.2; HRMS calculated: 427.1468, found: 427.147.

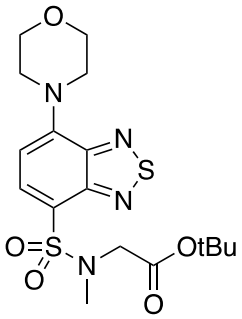

Synthesis of 5a. 0.2 mmol scale yielding an orange solid (84 mg, quantitative yield). ^{1}H NMR (500 MHz, $CDCl_3$) δ 1.34 (s, 9H), 2.96 (s, 3H), 3.78 (t, *J* = 4.85 Hz., 4H), 3.98 (t, *J* = 4.55 Hz., 4H) 4.17 (s, 2H) 6.66 (d, *J* = 8.2 Hz., 1H), 8.11 (d, *J* = 8.15 Hz., 1H); ^{13}C NMR (125 MHz, $CDCl_3$) δ 28.0, 35.6, 49,6, 52.1, 66.7, 82.0, 107.6, 121.1, 134.4, 147.1, 148.1, 151.8, 168.3; HRMS calculated: 451.1080 (M+Na), found: 451.1085.

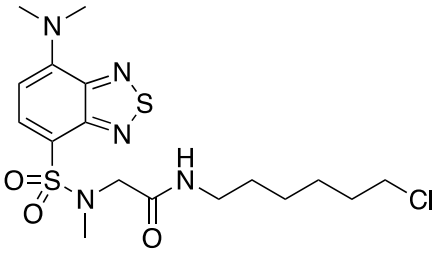

Synthesis of 1. Representative procedure. Compound **1a** (0.12 mmol, 50 mg) was dissolved in 20% Trifluoroacetic acid in dichloromethane and stirred at ambient temperature for 1 hour. Upon TLC verification of reaction completion, the solution was concentrated, redissolved in 1 mL of dichloromethane, and concentrated again. This process was repeated 3 times to ensure the removal of excess trifluoroacetic acid. The resulting oil was dissolved in anhydrous tetrahydrofuran (2.5 mL) and cooled to 0 °C. N-methylmorpholine (0.65 mmol, 71 µL) was added followed by isobutylchloroformate (0.13 mmol, 17 µL) dropwise. The resulting solution was stirred at 0 °C for 15 minutes, after which 6-chlorohexylamine·HCl (66 mg, 0.39 mmol) was added in one portion. The solution was allowed to stir at 0 °C to room temperature for 18 hours, after which, the solution was filtered, and the filtrate concentrated. The crude oil was purified by silica gel chromatography to yield the target compound as an orange solid (42 mg, 74% yield). ^{1}H NMR (500 MHz, $CDCl_3$); δ 1.37 (m, 2H), 1.47 (m, 2H), 1.59 (m, 2H), 1.78 (m, 2H), 2. 82 (s, 3H), 3.35 (m, 2H), 3.52 (m, 8H), 4.05 (s, 2H), 6.38 (d, *J* = 8.6 Hz., 1H), 7.37 (s, 1H), 8.12 (d, *J* = 8.55 Hz., 1H). ^{13}C NMR (125 MHz, $CDCl_3$) δ 26.15, 26.52, 29.46, 32.43, 36.8, 39.29, 42.89, 44.99, 54.16, 103.34, 112.67, 136.94, 147.23, 147.71, 152.22, 168.66; HRMS calculated: 448.1238, found: 448.1250.

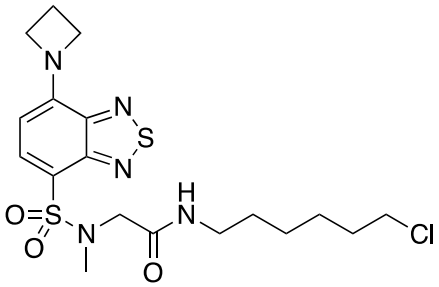

Synthesis of 2. 0.2 mmol scale yielding an orange solid (62 mg, 62% yield). ^{1}H NMR (500 MHz, $CDCl_3$) δ 1.34 (m, 2H), 1.46 (m, 2H), 1.56 (m, 2H), 1.77 (m, 2H), 2.12 (m, 4H), 2.81 (s, 3H), 3.31 (q, *J* = 6.85 Hz, 2H), 3.52 (t, *J* = 6.65, 2H), 3.96 (s, 3H), 6.23 (d, *J* = 8.6 Hz., 1H), 7.17 (s, 1H), 8.10 (d, *J* = 8.55 Hz., 1H); ^{13}C NMR (125 MHz, $CDCl_3$) δ 25.5, 26.1, 26.5, 28.2, 29.5, 32.4, 36.8, 39.3, 44.9, 51.0, 54.1, 101.9, 110.7, 137.4, 144.8, 147.6, 152.2, 168.8; HRMS calculated: 460.1238, found: 460.1251.

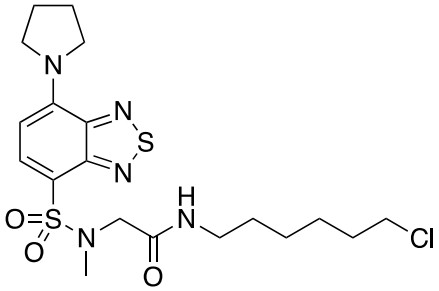

Synthesis of 3. 0.12 mmol scale yielding an orange solid (40 mg, 71% yield). ^{1}H NMR (500 MHz, $CDCl_3$) δ 1.36 (m, 2H), 1.48 (m, 2H), 1.57 (m, 2H), 1.77 (m, 2H), 2.24 (m, 2H), 2.85 (s, 3H), 3.33 (m, 2H), 3.53 (t, *J* = 6.65 Hz., 2H), 3. 68 (t, *J* = 6.6 Hz., 2H), 3. 71 (t, *J* = 5.95 Hz., 2H), 3.99 (s, 2H), 6.02 (s, 1H), 6.45 (d, *J* = 8.3 Hz., 1H), 7.11 (s, 1H), 8.17 (d, *J* = 8.2 Hz., 1H) ; ^{13}C NMR (125 MHz, $CDCl_3$) δ 26.1, 26.5, 29.4, 32.4, 36.8, 39.3, 44.9, 51.0, 54.1, 101.9, 110.8, 137.4, 144.8, 147.6, 152.3, 168.9 ; HRMS calculated: 474.1395, found: 474.1408.

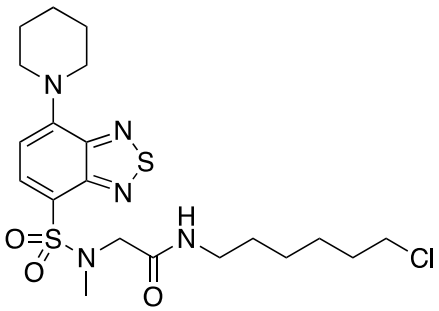

Synthesis of 4. 0.11 mmol scale to yield an orange solid (52 mg, quantitative yield). ^{1}H NMR (500 MHz, $CDCl_3$) δ 1.35 (m, 2H), 1.44 (m, 2H), 1.55 (m, 2H), 1.77 (m, 8H), 2.82 (s, 3H), 3.30 (q, *J* = 6.8 Hz., 2H), 3.51 (t, *J* = 6.7 Hz., 2H), 3.87 (m, 4H), 3.96 (s, 2H), 6.61 (d, *J* = 8.45 Hz., 1H), 7.02 (t, 5.1 Hz., 1H), 8.11 (d, *J* = 8.4 Hz., 1H); ^{13}C NMR (125 MHz, $CDCl_3$) δ 24.3, 25.7, 26.1, 26.4, 29.4, 29.6, 32.3, 36.7, 39.2, 44.9, 50.7, 54.1, 106.4, 136.6, 147.9, 148.5, 151.9, 168.5 ; HRMS calculated: 488.1551, found: 488.1566.

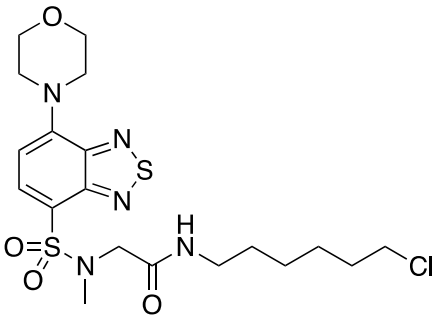

Synthesis of 5. 0.11 mmol scale to yield an orange solid (52 mg, quantitative yield). ^{1}H NMR (500 MHz, $CDCl_3$) δ 1.35 (m, 2H), 1.46 (m, 2H), 1.56 (m, 2H), 1.75 (m, 2H), 2.85 (s, 3H), 3.3 (q, *J* = 6.7 Hz., 2H), 3.52 (t, *J* = 5 Hz., 4H), 3.96 (m, 6H), 6.66 (d, *J* = 8.35 Hz., 1H), 6.94 (m, 1H), 8.15 (d, *J* = 8.25 Hz., 1H); ^{13}C NMR (125 MHz, $CDCl_3$) δ 26.2, 26.6, 29.5, 36.9, 39.4, 45.0, 49.6, 54.4, 66.7, 107.1, 117.5, 136.3, 147.6, 148.6, 151.8, 168.5; HRMS calculated: 490.1344, found: 490.1362.

NMR Spectra

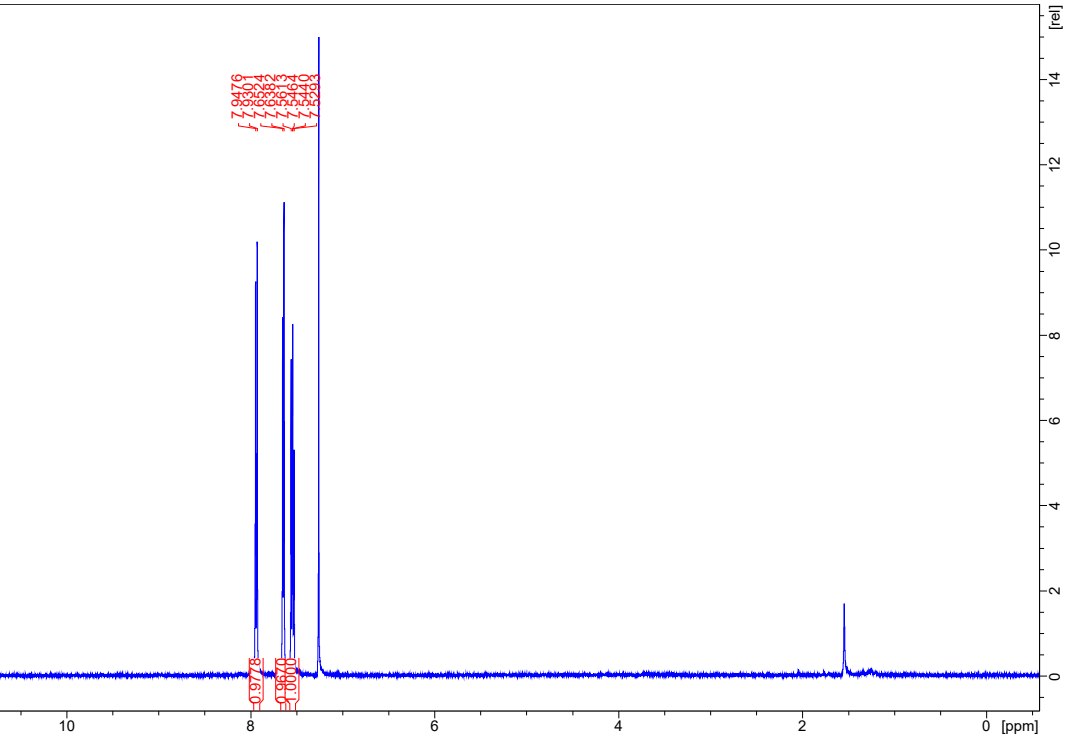

Figure S12. ^{1}H NMR spectra of **10** in $CDCl_3$

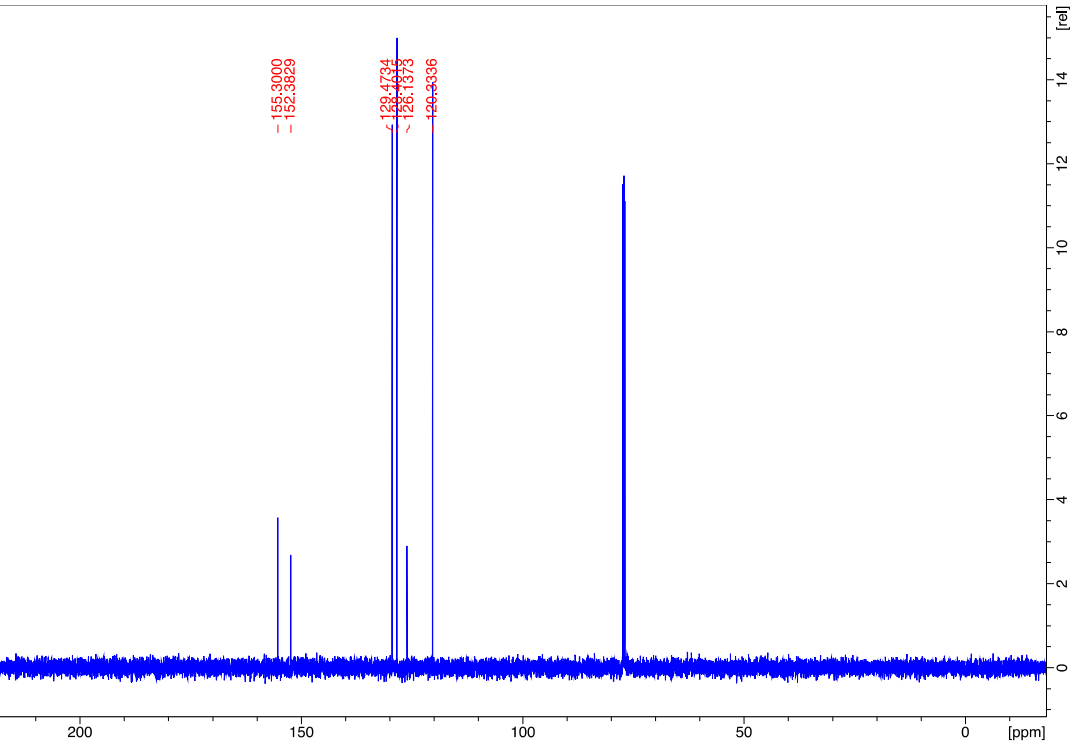

Figure S13. ^{13}C NMR spectra of **10** in $CDCl_3$

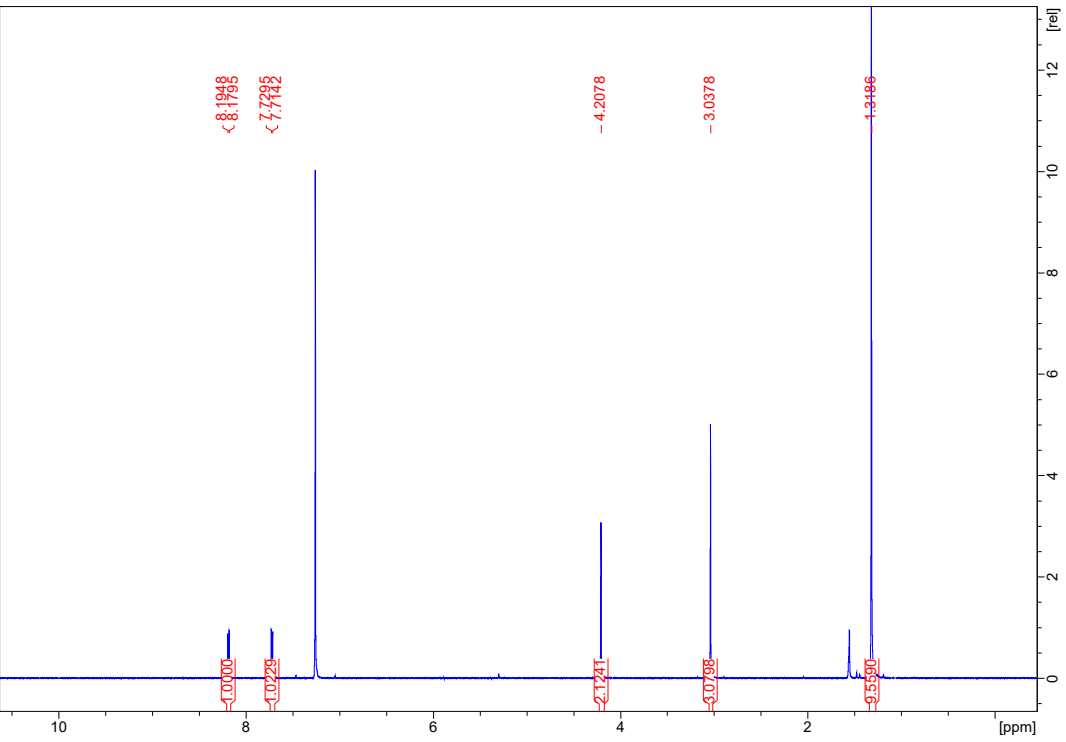

Figure S14. ^{1}H NMR spectra of **12** in $CDCl_3$

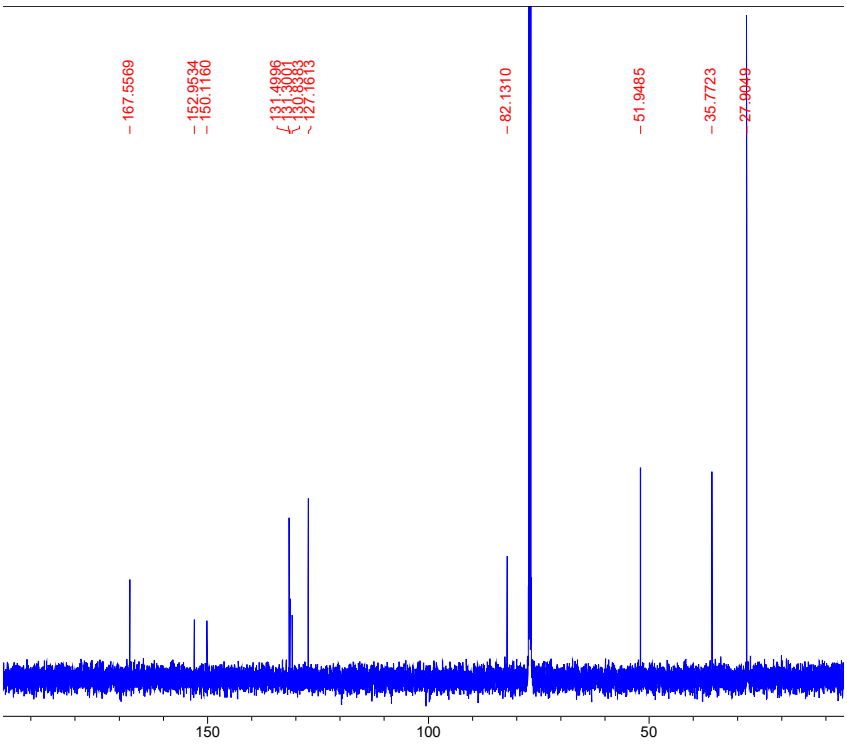

Figure S15. ^{13}C NMR of **12** in $CDCl_3$.

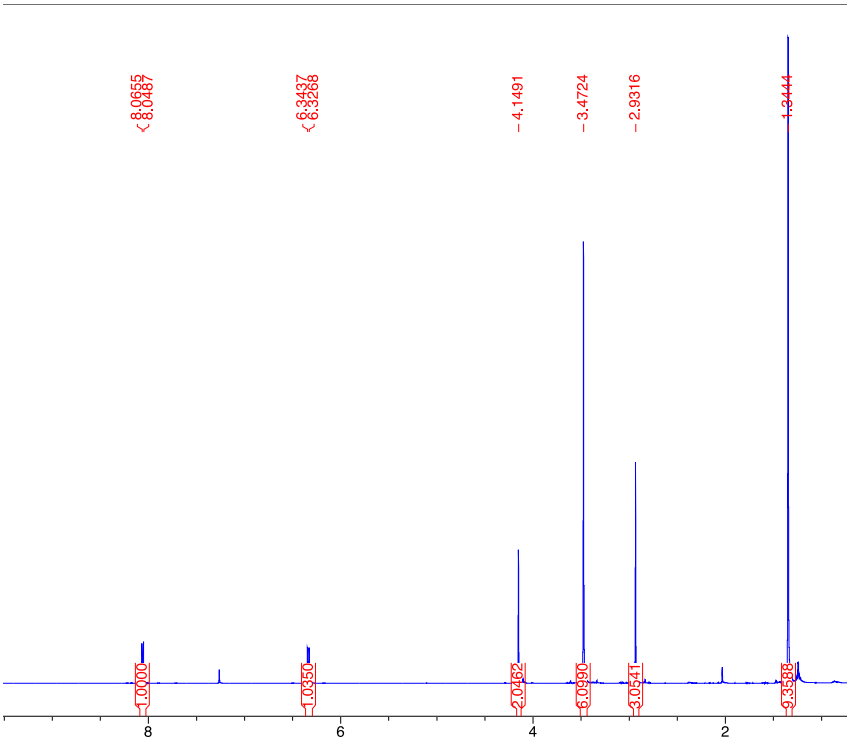

Figure S16. ^{1}H NMR of **1a** in $CDCl_3$.

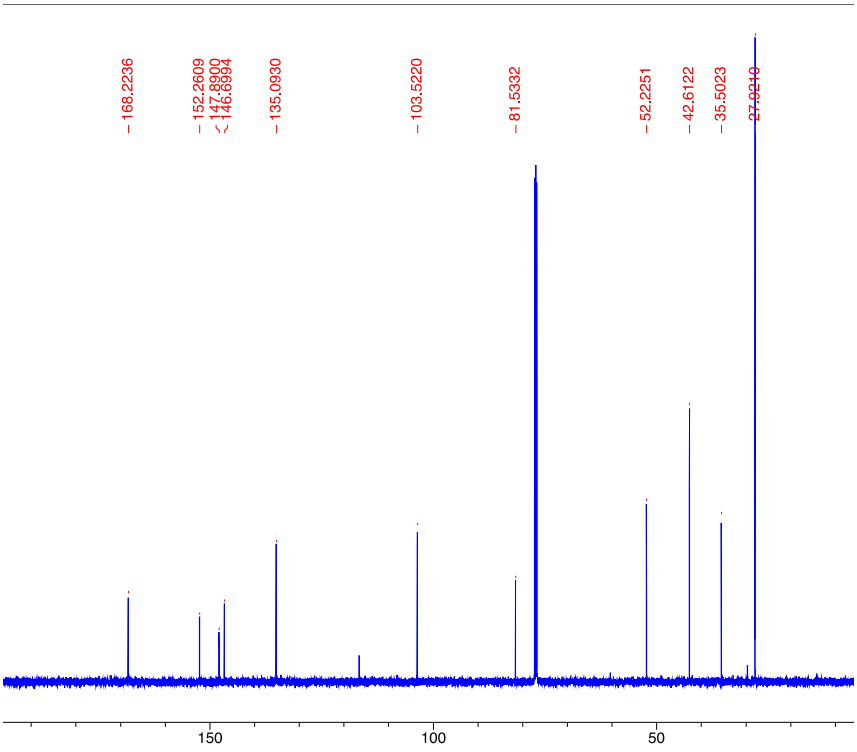

Figure S17. ^{13}C NMR spectra of **1a** in $CDCl_3$

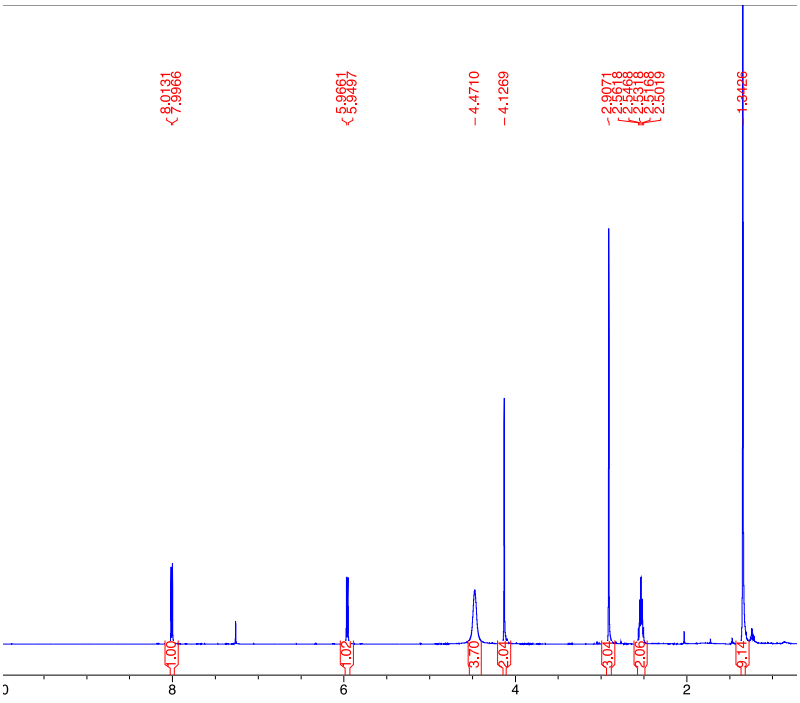

Figure S18. ^{1}H NMR spectra of **2a** in $CDCl_3$.

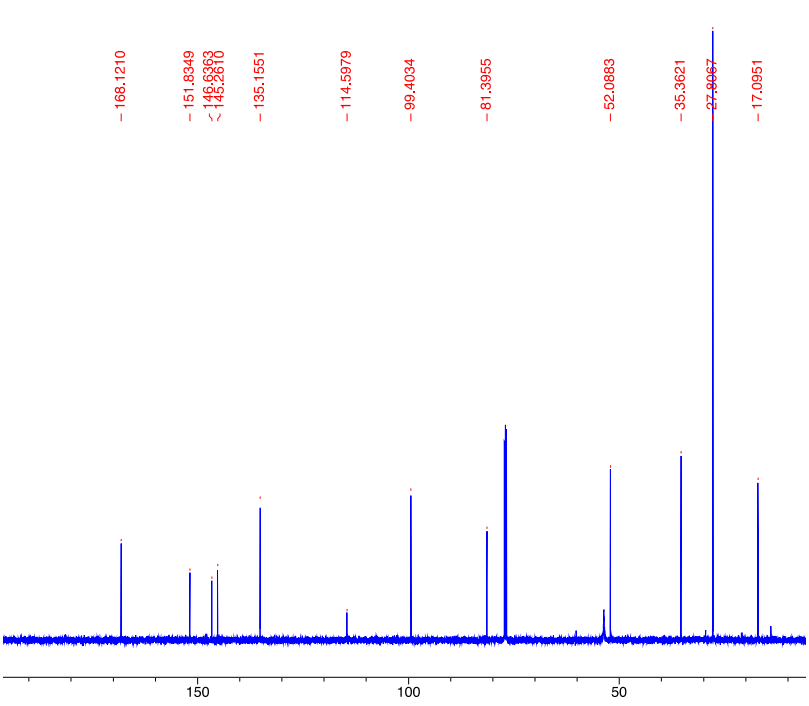

Figure S19. ^{13}C NMR spectra of **2a** in $CDCl_3$

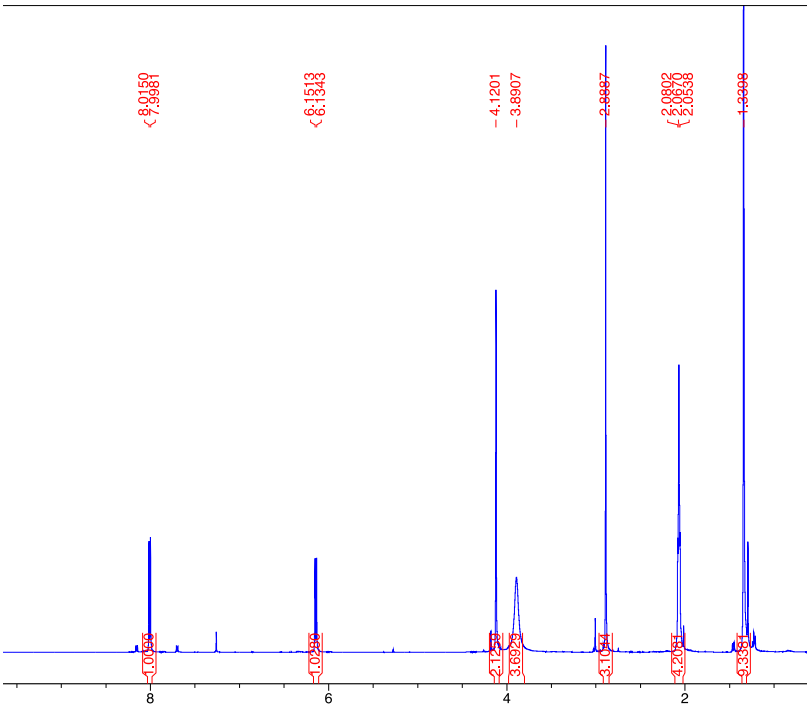

Figure S20. ^{1}H NMR spectra of **3a** in $CDCl_3$.

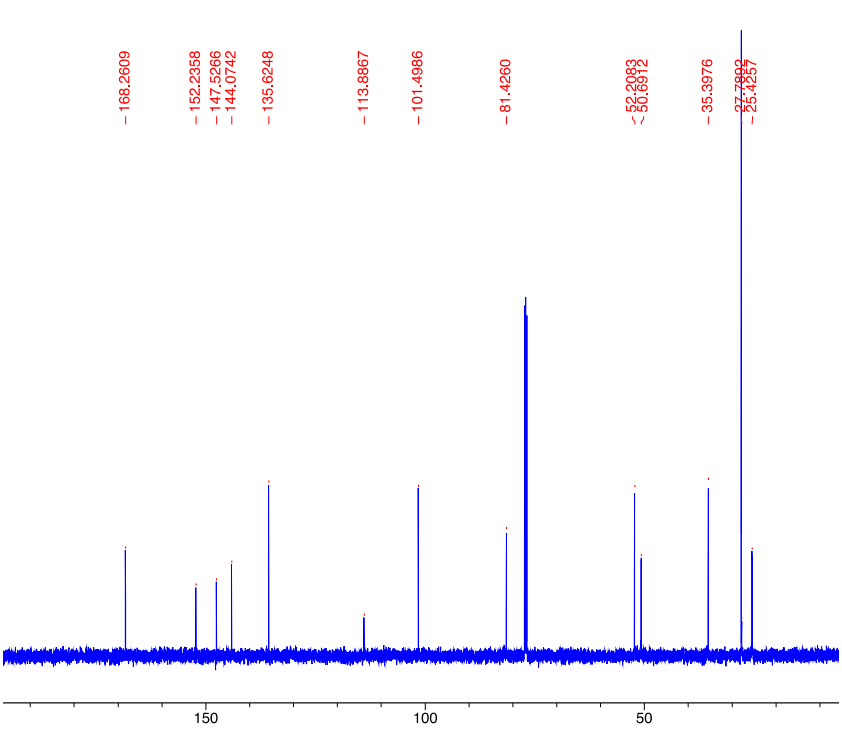

Figure S21. ^{13}C NMR spectra of **3**a in $CDCl_3$

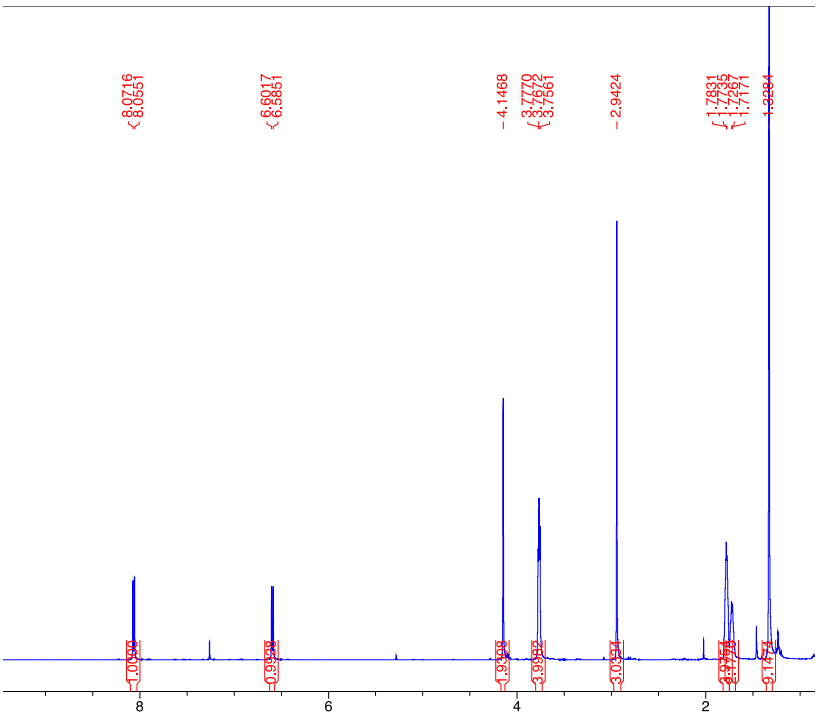

Figure S22. ^{1}H NMR spectra of **4a** in $CDCl_3$.

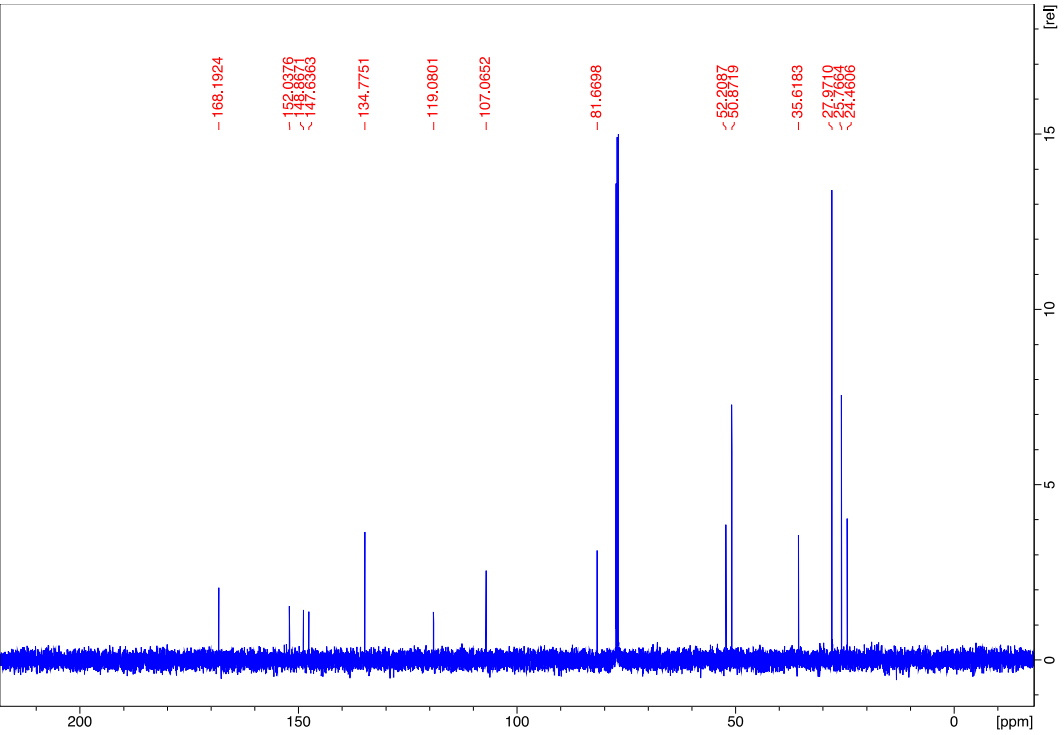

Figure S23. ^{13}C NMR spectra of **4a** in $CDCl_3$.

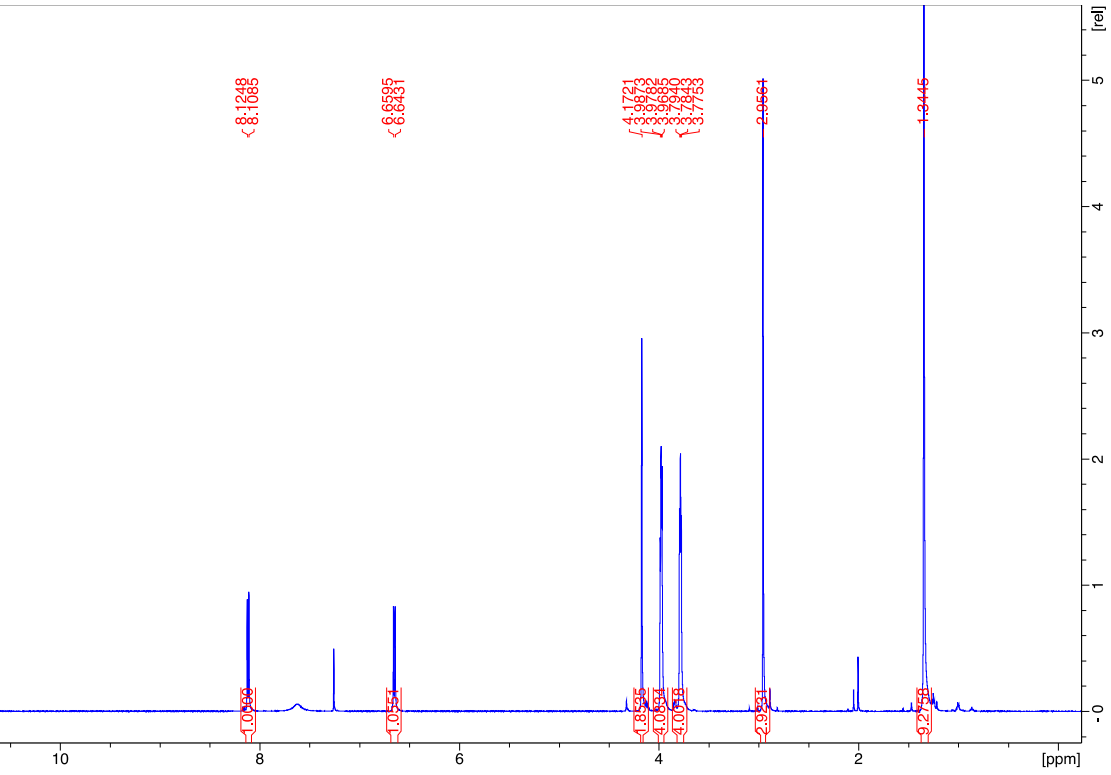

Figure S24. ^{1}H NMR spectra of **5a** in $CDCl_3$.

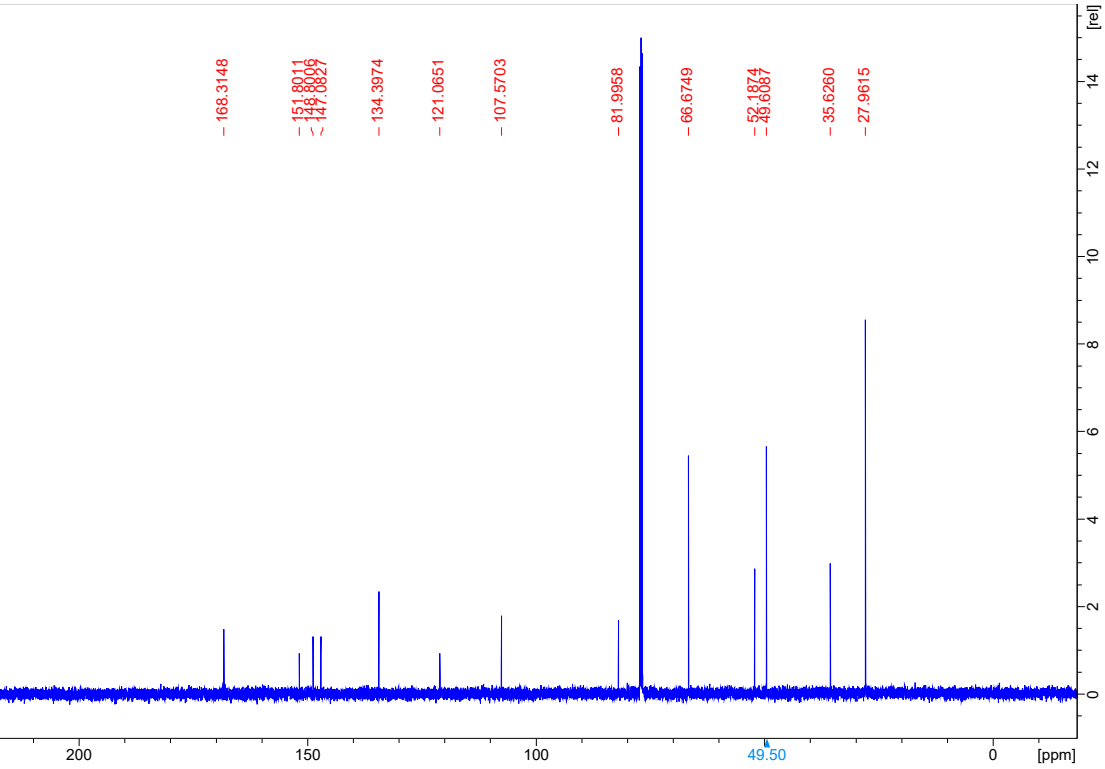

Figure S25. ^{13}C NMR spectra of **5a** in $CDCl_3$.

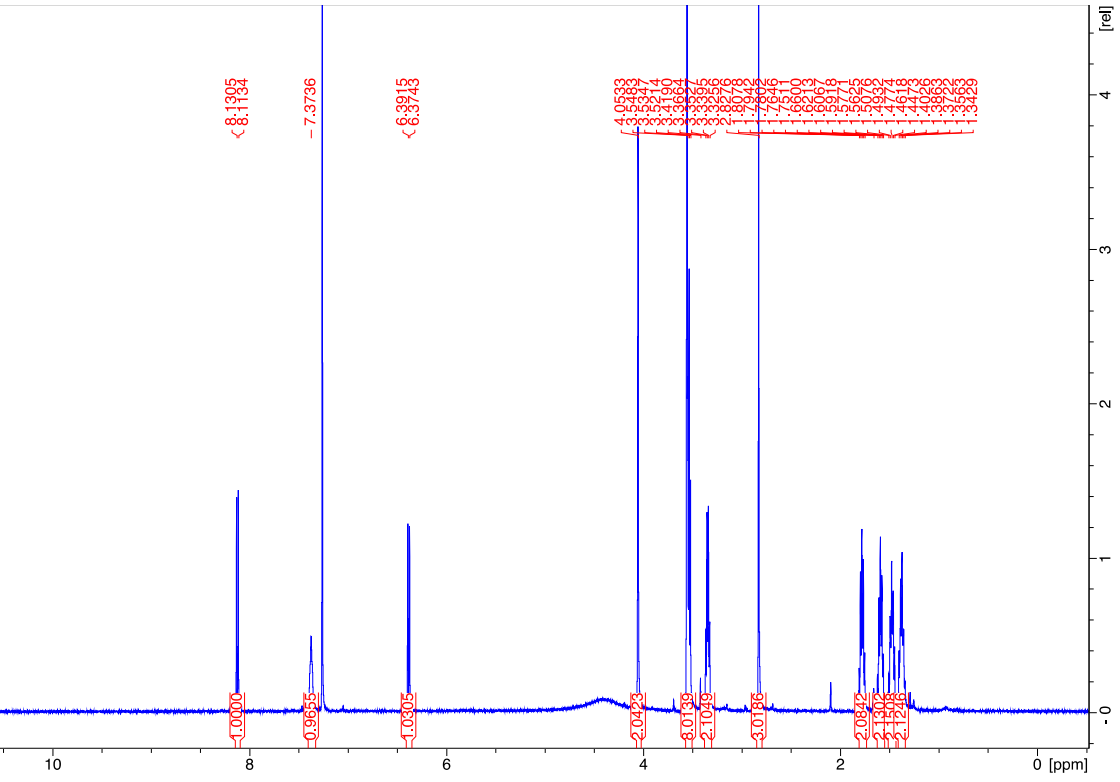

Figure S26. ^{1}H NMR spectra of **1** in $CDCl_3$.

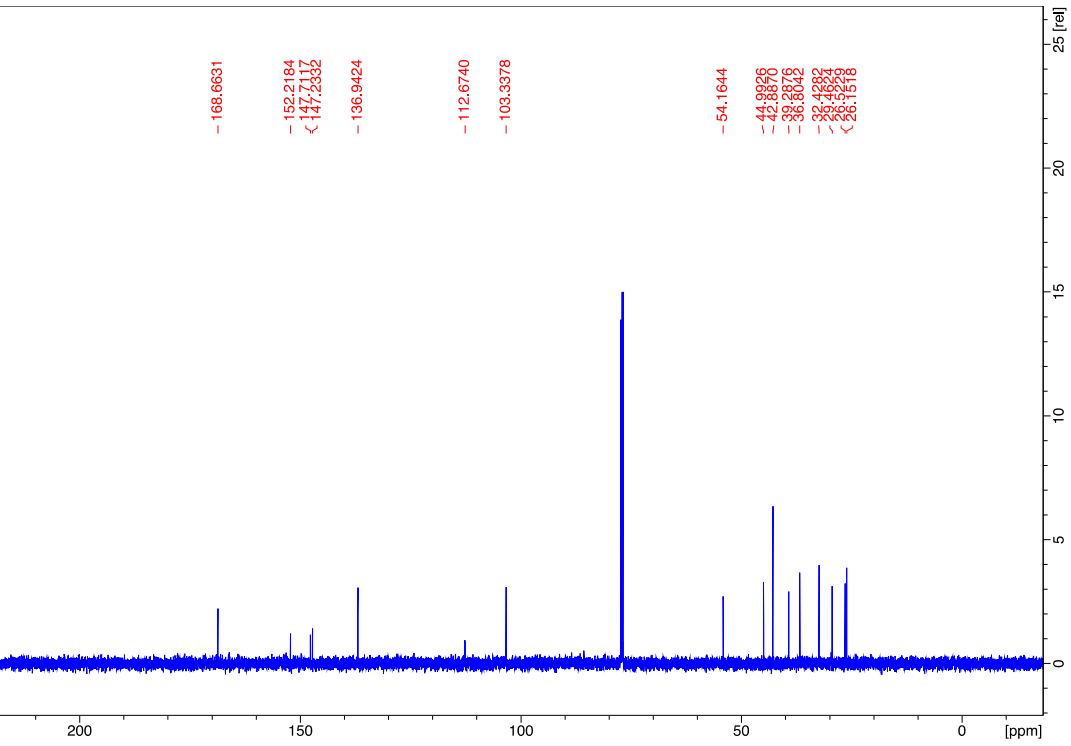

Figure S27. ^{13}C NMR spectra of **1** in $CDCl_3$.

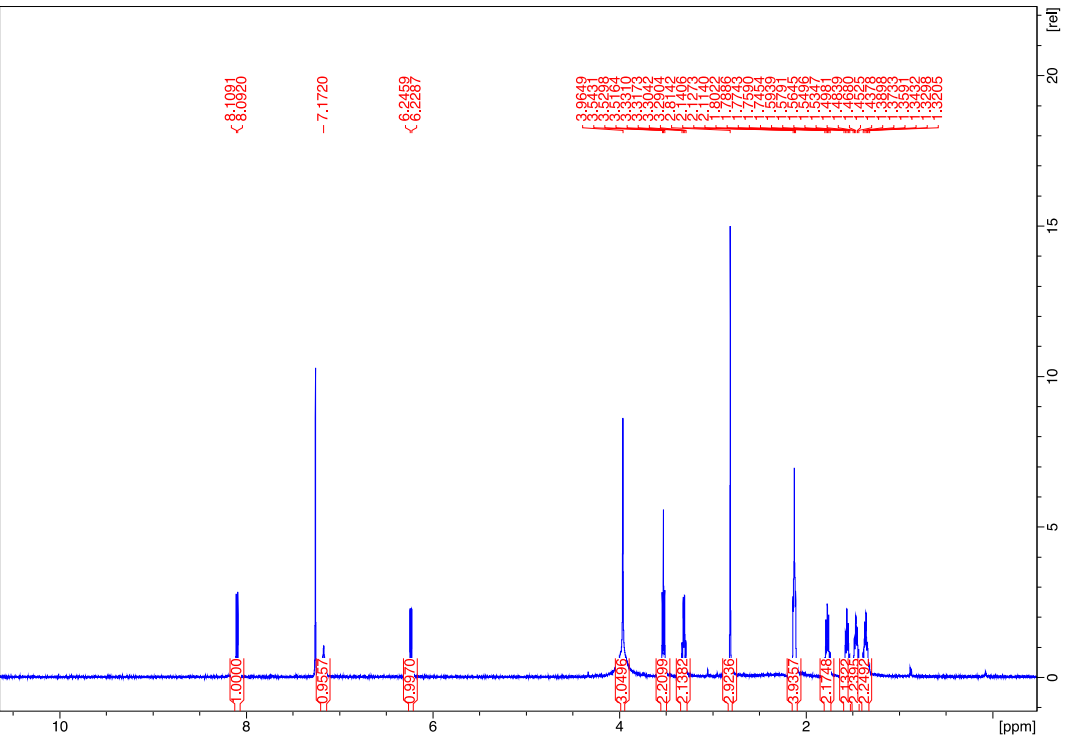

Figure S28. ^{1}H NMR spectra of **2** in $CDCl_3$.

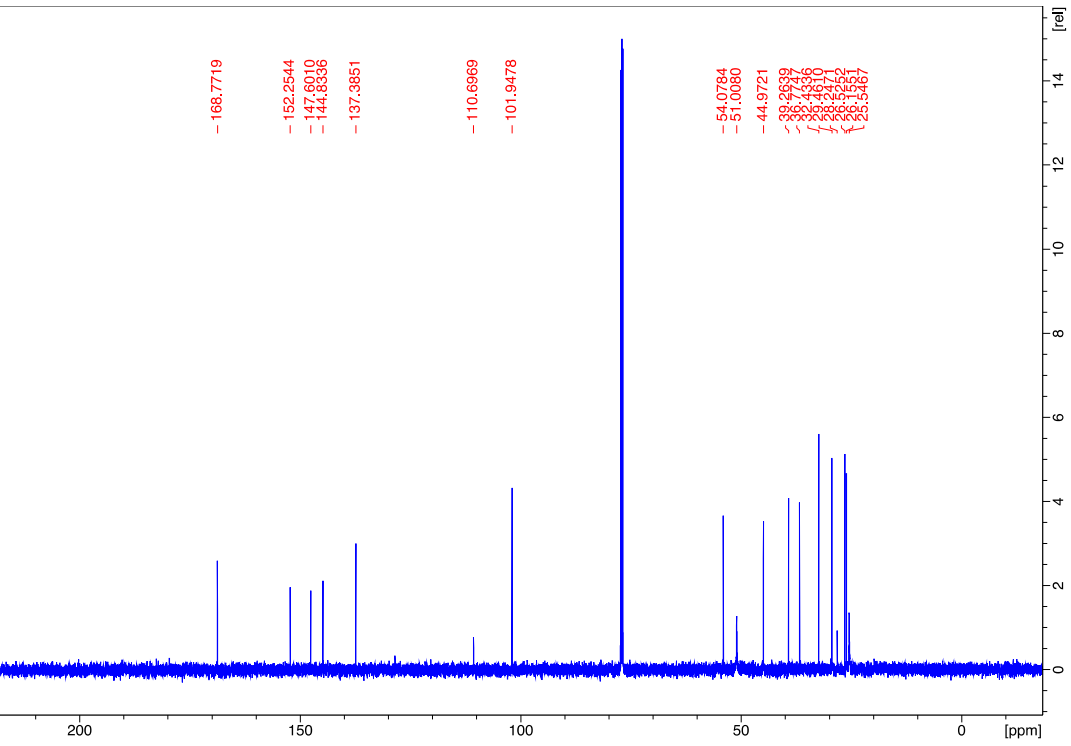

Figure S29. ^{13}C NMR spectra of **2** in $CDCl_3$.

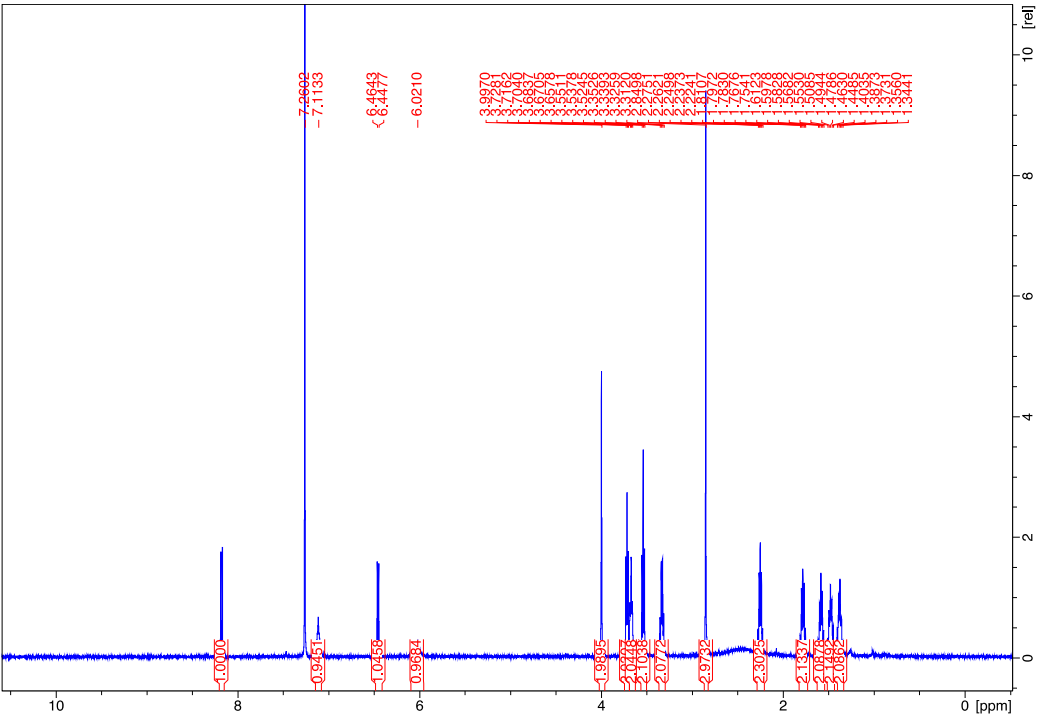

Figure S30. ^{1}H NMR spectra of **3** in $CDCl_3$.

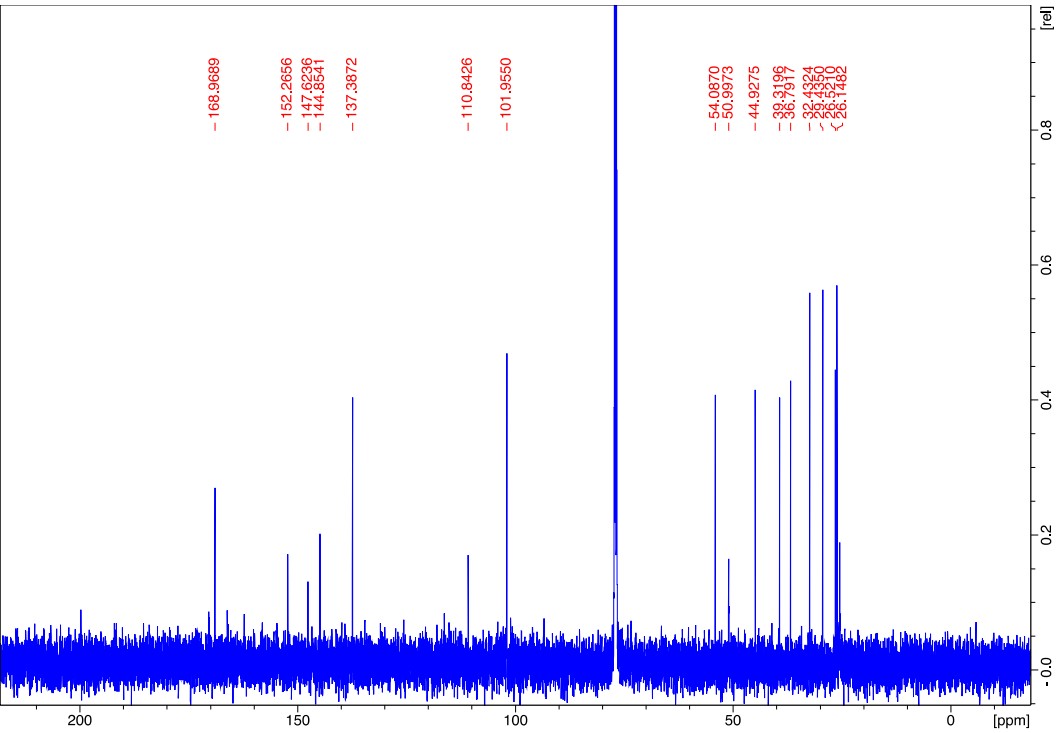

Figure S31. ^{13}C NMR spectra of **3** in $CDCl_3$.

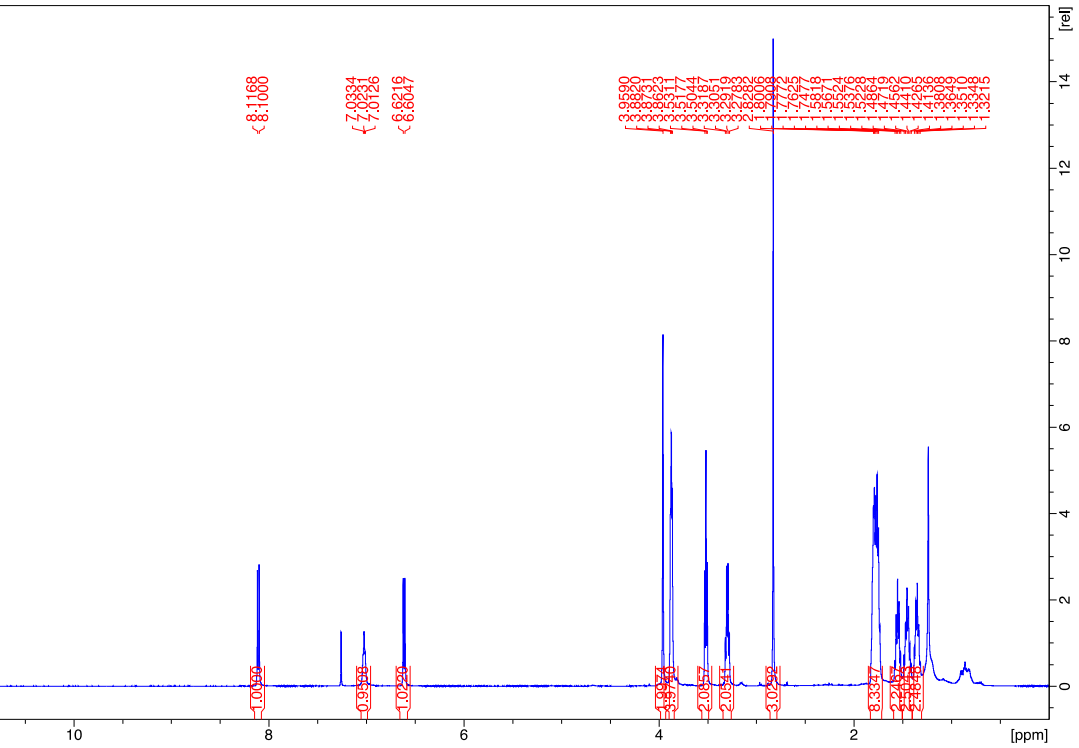

Figure S32. ^{1}H NMR spectra of **4** in $CDCl_3$.

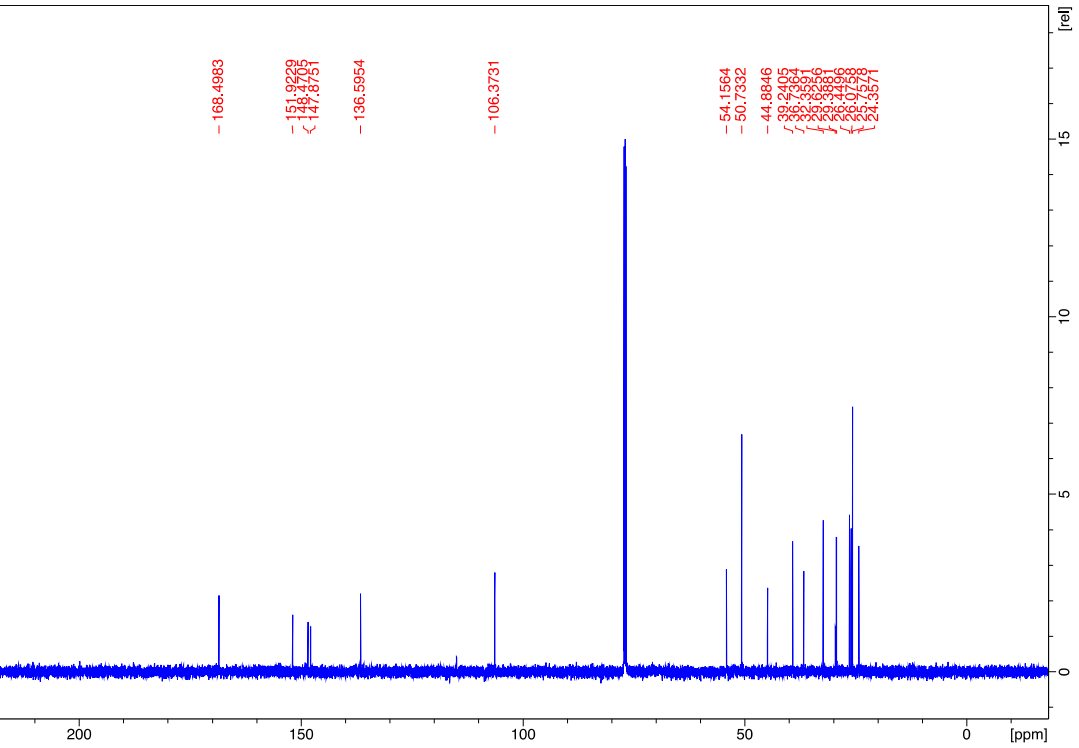

Figure S33. ^{13}C NMR spectra of **4** in $CDCl_3$.

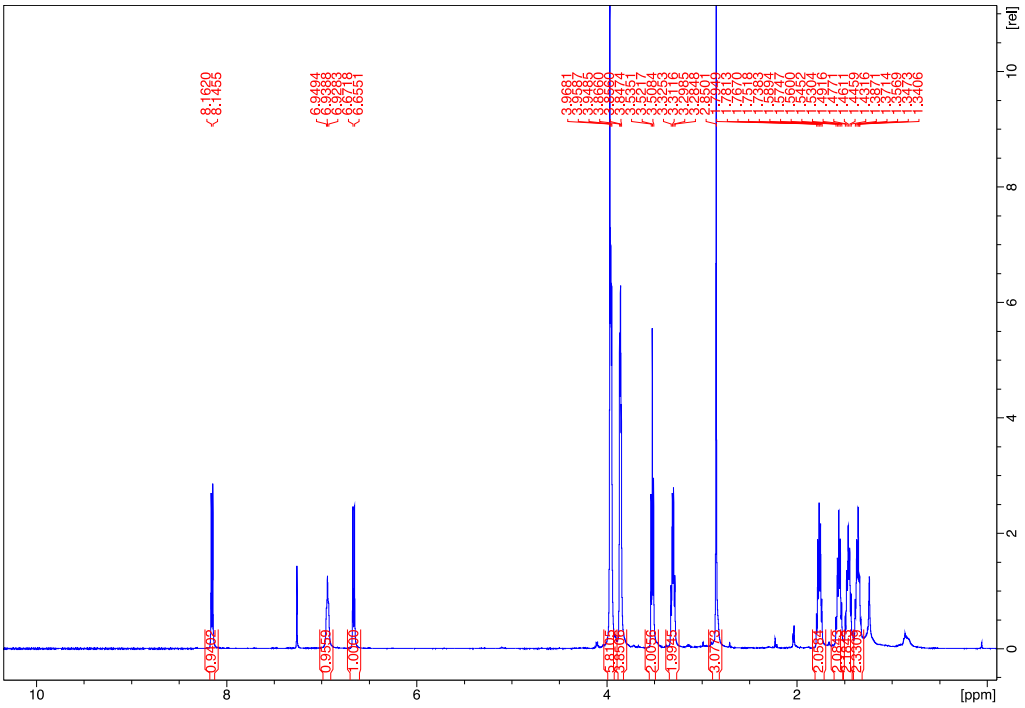

Figure S34. ^{1}H NMR spectra of **5** in $CDCl_3$.

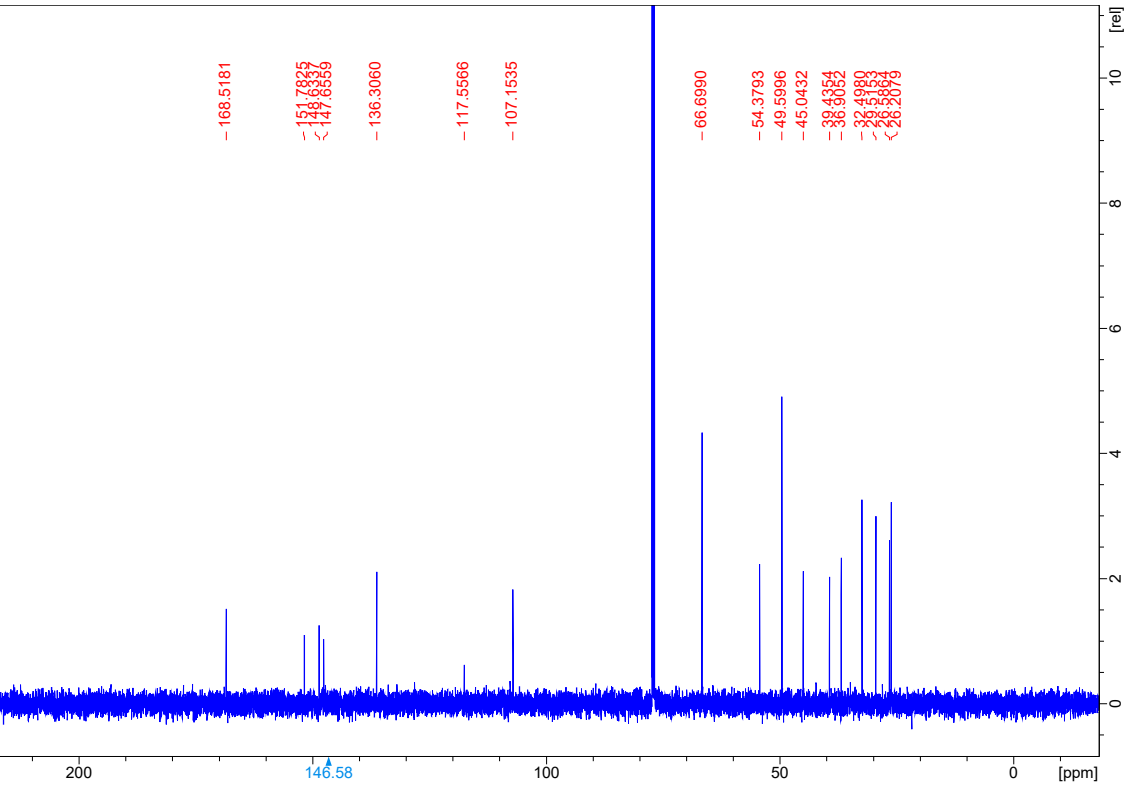

Figure S35. ^{13}C NMR spectra of **5** in $CDCl_3$.

References

(1) Grimm, J. B.; English, B. P.; Chen, J.; Slaughter, J. P.; Zhang, Z.; Revyakin, A.; Patel, R.; Macklin, J. J.; Normanno, D.; Singer, R. H.; Lionnet, T.; Lavis, L. D. A General Method to Improve Fluorophores for Live-Cell and Single-Molecule Microscopy. *Nat. Methods* **2015**, *12* (3), 244–250. https://doi.org/10.1038/nmeth.3256.

(2) Ye, Z.; Yang, W.; Wang, C.; Zheng, Y.; Chi, W.; Liu, X.; Huang, Z.; Li, X.; Xiao, Y. Quaternary Piperazine-Substituted Rhodamines with Enhanced Brightness for Super-Resolution Imaging. *J. Am. Chem. Soc.* **2019**, *141* (37), 14491–14495. https://doi.org/10.1021/jacs.9b04893.

(3) Aue, D. H.; Webb, H. M.; Bowers, M. T. Quantitative Proton Affinities, Ionization Potentials, and Hydrogen Affinities of Alkylamines. *J. Am. Chem. Soc.* **1976**, *98* (2), 311–317. https://doi.org/10.1021/ja00418a001.

(4) Yoshikawa, K.; Hashimoto, M.; Morishima, I. Photoelectron Spectroscopic Study of Cyclic Amines. Relation between Ionization Potentials, Basicities, and s Character of the Nitrogen Lone Pair Electrons. *J. Am. Chem. Soc.* **1974**, *96* (1), 288–289. https://doi.org/10.1021/ja00808a066.

(5) Colonna, F. P.; Distefano, G.; Pignataro, S.; Pitacco, G.; Valentin, E. Ionization Energies of Some Amines and Enamines and an Estimation of Their Relative Basicity in Gaseous Phase. *J. Chem. Soc. Faraday Trans. 2 Mol. Chem. Phys.* **1975**, *71* (0), 1572–1576. https://doi.org/10.1039/F29757101572.
(6) Deprey, K.; Kritzer, J. A. HaloTag Forms an Intramolecular Disulfide. *Bioconjug. Chem.* **2021**, *32* (5), 964–970. https://doi.org/10.1021/acs.bioconjchem.1c00113.
(7) Liu, Y.; Miao, K.; Dunham, N. P.; Liu, H.; Fares, M.; Boal, A. K.; Li, X.; Zhang, X. The Cation−π Interaction Enables a Halo-Tag Fluorogenic Probe for Fast No-Wash Live Cell Imaging and Gel-Free Protein Quantification. *Biochemistry* **2017**, *56* (11), 1585–1595. https://doi.org/10.1021/acs.biochem.7b00056.